User-driven applications and tools for Climate-Informed Maritime Spatial Planning and integrated seascape management, towards a resilient & inclusive Blue Economy

D3.1 – Data harmonization, federation and exchange framework

WP3 – Core technology modules for data & services federation and curation

Project funded from the EU HE research and innovation programme
under GA No. 101112919

Lead Contributors	Ioannis Kavouras (ICCS)
Other Contributors	IN2, WTOC, CREO
Reviewers	Joris Jaruschewski (OHB), Daphne Pantousa (RG), Eirini Marinou (GSH), Natalia Czortek (CREO), Platon Patlakas (HCMR)

Due Date	31.07.2025
Delivery Date	**31.07.2025 [M20]**
Type	Document, Report
Dissemination Level	PU - Public

Keywords	Data harmonization, Exchange framework, OCEANIDS Data Cubes, GeoServer

Document History

Version	Date	Description	Reason for Change	Distribution
0.1	25/05/2025	1st Draft	-	ICCS
0.2	05/06/2025	2nd Draft	Proofreading and editing	ICCS
0.3	17/06/2025	1st Final Version	Proofreading and editing	ICCS
0.4	01/07/2025	3rd Draft	Sent for adjustments	GSH
0.5	15/07/2025	4th Draft	Review	HCMR, OHB, RG
0.6	28/07/2025	5th Draft	Updates from the review	ICCS
1.0	31/07/2025	Final	Submission	GSH

Legal Disclaimer

Table of Contents

Executive Summary 5
List of Tables 6
List of Figures 6
1 Introduction 9
1.1 Scope and Objective of the Deliverable 10
1.2 Structure of the Deliverable 10
1.3 Relation to other projects and tasks 11
2 The OCEANIDS Data Cubes Framework Architecture and Comparison with the Literature Data Cubes 12
2.1 Existing Earth Observation Data Cubes Implementations 13
2.2 The OCEANIDS Data Cubes framework 14
2.2.1 OCEANIDS Climate/Meteorological Data Cubes Description 18
2.2.2 OCEANIDS Earth Observation Data Cubes Description 24
3 ODC Data Storage and Exchange Framework 35
3.1 Data Storage Management 36
3.2 Data Exchange via sFTP transfer 36
3.3 Data Exchange via GeoServer 37
4 Demonstration of ODC Applications 40
4.1 Disaster monitoring in coastal areas - Monitoring the oil-spill disaster in Saronikos Gulf in September 2017 40
4.2 Monitoring port degradation parameters – Monthly monitoring of Crete and Port of Heraklion area from January 2016 to December 2024 42
4.2.1 Results 45
4.2.2 Discussion 53
5 Conclusions 54
References 55

Executive Summary

This deliverable **D3.1 "Data harmonization, federation and exchange framework"** outlines the data harmonization, federation, and exchange framework developed under Task 3.1 "Data harmonization (OCEANIDS Data Cubes), federation and exchange framework for increased data consumption" led by ICCS, which is part of the WP3 "Core technology modules for data & services federation and curation" led by HCMR, of the OCEANIDS project. Its primary objective is to establish a robust, interoperable system for managing heterogeneous EO (Earth Observation) and climate datasets to support user-driven applications for climate-informed maritime spatial planning and integrated seascape management.

To address the challenges of fragmented data formats, resolutions, and sources, the report introduces the OCEANIDS Data Cubes Framework, a backend solution for generating harmonized, analysis-ready data cubes. The framework supports both EO (e.g., Sentinel and Landsat missions) and non-EO data (e.g., CORDEX climate projections), enabling multi-source, multi-dimensional spatiotemporal analysis. Key technical features include spatial harmonization, reprojection, clipping, and the calculation of spectral indices, with outputs standardized in NetCDF format for wide compatibility.

The document compares the OCEANIDS framework to existing data cube implementations, detailing its novel contributions in terms of flexibility, multi-resolution support, and post-processing adaptability. It also explains data storage optimization strategies and data sharing mechanisms through sFTP and GeoServer, ensuring both efficient consortium collaboration and end-user accessibility via standard services (e.g., WMS/WFS).

List of Tables

Table 1. List of Acronyms/Abbreviations....8
Table 2. CORDEX dataset for the OCEANIDS project....19
Table 3. EURO CORDEX Parameters[36]....23
Table 4. EO Data Sources....24
Table 5. The ODC products....31
Table 6. Storage Ratio Metric for Clipping with Port of Heraklion geometry ODC products.....47
Table 7. Storage Ratio Metric for Clipping with Crete geometry ODC products.....47

List of Figures

Figure 1. OCEANID'S WPs structure workflow....11
Figure 2. An example of a Data Cube's dimension expanding....12
Figure 3. The OCEANIDS Data Cubes' architecture and framework workflow....15
Figure 4. Parameters of the CORDEX rotated coordinates....23
Figure 5. EURO CORDEX Domain[36]....23
Figure 6. The workflow of ODC EO Services....28
Figure 7. WP3 overall architecture.....35
Figure 8. Direct connection between T3.1, T3.5 and WP4.....36
Figure 9. Data Exchange via sFTP transfer using FileZilla....37
Figure 10. Example of a Sentinel-2 product inside the GeoServer. In this example the NDVI and NDWI layers have been created for distribution.....37
Figure 11. New Layer creation panel inside the GeoServer. This is an administrative page, which allows the creation and distribution of layers.....38
Figure 12. Visualization of NDVI layer inside GeoServer....38
Figure 13. Visualization of GeoServer's NDVI layer inside QGIS and overlayed over Google Maps basemap.....39
Figure 14. Time series monitoring the water quality of Saronikos gulf before and after the oil-spill using the RGB, NDWI, WRI and OSI products of the ODC framework. The green box indicates the critical area of identified oil-spill.....41
Figure 15. Polygon geometries of selected areas of interest. (a) Red boundary is used for clipping the whole Crete Island; (b) Yellow boundary is used for clipping the coastal area around the Port of Heraklion.....43
Figure 16. 5D (3 spatial, 1 temporal, and 1 spectral) visualization of the NDVI difference in Port of Heraklion from February 2019 to February 2020.....44
Figure 17. Samples of 4D (***time x bands x lat x lon***) analysis using ODC products for the Port of Heraklion. (a) Visible Spectrum; (b) Visible Near Infrared; (c) Visible Short-ware

Infrared; (d) Normalized Difference Vegetation Index; (e) Normalized Difference Water Index; (f) Normalized Difference Build-up Index. 46
Figure 18. Example of periodic monitoring in coastal area of Port of Heraklion, using a yearly temporal window near February each year. The yellow boundary indicates critical condition and possible degradation in the coastal area. 48
Figure 19. Comparison between the products of February 26th, 2022 (critical conditions) and February 21st, 2023 (normal conditions). 50
Figure 20. 5D visualization of ODC products inside QGIS. 51
Figure 21. Land Surface Temperature 4D monitoring using Landsat-8/9 products. 52

Table 1. List of Acronyms/Abbreviations

Acronym Abbreviation	Explanation
CAP	Climate Adaptation Planning
CC	Climate Change
C3S	Copernicus Climate Change Service
CI-MSP	Climate-Informed Maritime Spatial Planning
CORDEX	Coordinated Regional Climate Downscaling Experiment
CRS	Coordinate Reference System
DC	Data Cube
DEMs	Digital Elevation Models
DSS	Decision Support System
DTMs	Digital Terrain Models
EO	Earth Observation
ESA	European Space Agency
EWS	Early Warning System
GA	Grand Agreement
GIS	Geographical Information Systems
HCMR	Hellenic Centre for Marine Research
ICCS	Institute of Communication and Computer Systems
NDVI	Normalized Difference Vegetation Index
NetCDF	Network Common Data Form
ODC	OCEANIDS Data Cube
O-DSP	OCEANIDS Decision Support Platform
OLAP	Online Analytical Processing
QGIS	Quantum Geographic Information System
OSI	Oil Spill Index
PQR	Products Quality Resolution
RCMs	Regional Climate Models
RCP	Representative Concentration Pathway
sFTP	Secure File Transfer Protocol
SHP	Shapefiles
SR	Storage Ratio
TPR	Time Performance Ratio
USGS	United States Geological Survey
VRT	Virtual Raster
WMS	Web Map Service
WFS	Web Feature Service
WRI	Water Ratio Index

1 Introduction

OCEANIDS aims at building user-driven applications and tools, which act as an enabling technological layer for regional authorities and stakeholders to achieve a more resilient and inclusive systemic pathway to a Blue Economy in coastal regions. Bringing spatial and non-spatial data and services under a single-access window platform for Climate-Informed Maritime Spatial Planning (CI-MSP), the project will allow a more integrated seascape management of coastal regions. The project delivers a Decision Support tool (OCEANIDS Decision Support Platform - O-DSP), with an overarching target to collect, harmonize, and curate existing climate data services, making data accessible, reusable, and interoperable for the development of local adaptation strategies. Furthermore, CC (Climate Change) adaptation measures should consider local ecology, economy, society, politics, and technology. Therefore, the definition of Climate Adaptation Planning (CAP) must consider specific local socio-economic contexts. OCEANIDS facilitates access to knowledge, data, and digital services critically for better understanding and managing climate risks, enhancing adaptive capacities, and supporting transformative innovations.

The modern urban environments have been developed with the purpose of interconnecting people, infrastructures, activities, and several other resources, making them susceptible to environmental disasters and climate change effects[1],[2],[3]. Daily industrial activities, especially near the port areas, have a negative impact on the local environment and climate, endangering both human health and well-being, as well as the local nature species.

All human activities result in the following issues: (a) lack of urban greenness [4]; (b) flooding[5]; (c) non-healthy atmospheric quality[6]; (d) an increase of greenhouse gases emissions[7]; and (e) the phenomenon of heat island effect[8]. In most of these cases, the impact can be evaluated by continuously monitoring the activities over the area of interest using EO data provided by space-borne technologies (i.e., satellites) and aerial or in-field climate measurements. In other cases, the impact can be instantaneous, causing a large disaster over a radius, like in an oil spill situation.

Today, there is a large amount of EO data available, which expands each week [9]. In addition, the availability of data is produced from different providers (i.e., Copernicus, USGS, ESA, NASA, etc.), thus, there are differences in distribution format, spatial resolution, data collection, etc. In some cases, however, two missions from different providers (i.e., Landsat-8 from USGS and Sentinel-2 from Copernicus) have similarities. Such data can be used in combination for thickening an EO imagery time-series dataset.

A different category of data includes non-EO geolocated data, such as climate, meteorological, or seasonal time-series datasets. Such datasets are also provided by different sources, in a huge amount and storage size, which hinders their processing. However, such data can provide useful information (i.e., temperature, humidity, wind speed, etc.) in environmental and climate monitoring. Thus, they are a necessity for designing intelligent systems (i.e., EWS, DSS, etc.).

The collection of these data raises several Big Data challenges, such as data incompatibility, different formatting, different geolocation, different spatiotemporal windows, etc. The OCEANIDS project aims to improve the user-defined data manipulation tools, contributing to an ecosystem of readily available tools and integrated information services, both through

usage and further improvement. To achieve this, it is necessary to create a platform that harmonizes and mobilizes data from disparate data sources.

The OCEANIDS Data cubes framework falls under WP3, which consists of the following Tasks:

- **Task 3.1: "Data harmonization (OCEANIDS Data Cubes), federation and exchange framework for increased data consumption" [M1-M20]**
- Task 3.2: "New Earth observation (EO) data services requirements and specifications" [M1-M22]
- Task 3.3: "Climatic models and CC impact in coastal regions" [M1-M22]
- Task 3.4: "Meteorological models curation and quantitative environmental impact assessment in coastal regions" [M1-M32]
- Task 3.5: "Data validation for the integration into the C3S Climate Data Store (DIAS, Copernicus, ESA TEP, GEOSS, EMODNET and other EU research infrastructure)" [M10-M31]

This document is the report presenting the Data Cubes framework of the OCEANIDS project. It is the output of **Task 3.1: "Data harmonization (OCEANIDS Data Cubes), federation and exchange framework for increased data consumption" [M1 -M20]** and represents the first deliverable of WP3.

1.1 Scope and Objective of the Deliverable

Deliverable 3.1, entitled "Data harmonization, federation and exchange framework," integrates a backend framework for generating Data Cubes (DC) to address the Big Data challenges[10]. More specifically, D3.1 provides a workflow to achieve homogeneity among the various satellite and non-satellite data used in the OCEANIDS project. The development of services includes: **(a)** Data management and organization of data sources; **(b)** Integration, testing, running and management of application (processes); **(c)** Workflow definition via process chaining to produce the OCEANIDS Data Cube (ODC) products; **(d)** Systematic execution of workflows to enable utilization of scalable processing resources and process parallelization; **(e)** Visualization capabilities; and **(f)** Means of accessing delivered products.

1.2 Structure of the Deliverable

This document consists of the following chapters:

- **Chapter 2** includes general information regarding the OCEANIDS Data Cubes framework
- **Chapter 3** describes the ODC storage management and exchange framework
- **Chapter 4** presents demonstration examples of applications of ODCs
- **Chapter 5** summarises the conclusions of this deliverable

1.3 Relation to other projects and tasks

In the OCEANIDS project, the work packages are connected to providing robustness, interoperability, and interconnection between the different processes. Following the structure of the OCEANIDS project (**Figure 1**) the WP3 gets input from WP2. This input consists of information about the end-users (i.e., port authorities, policymakers, government, municipalities, etc.) and their ocean and maritime-related needs. This information provides the necessary foundation for WP3 to generate the low-level (back-end) tools, algorithms, and methodologies, as well as datasets to address these users' needs. The resulting outputs are then passed on to subsequent work packages, WP4 and WP5. This sequential structure ensures that each WP builds upon the inputs of its predecessor and delivers results to the next phase. Within this framework, the OCEANIDS Data Cubes (developed under Task 3.1) are part of WP3 and are responsible for pre-processing raw data and producing harmonized products aligned with common and open standards. These products are then used both by other tasks within WP3 and by the applications developed in WP4 and WP5, which further process and visualize the final outputs of the OCEANIDS project.

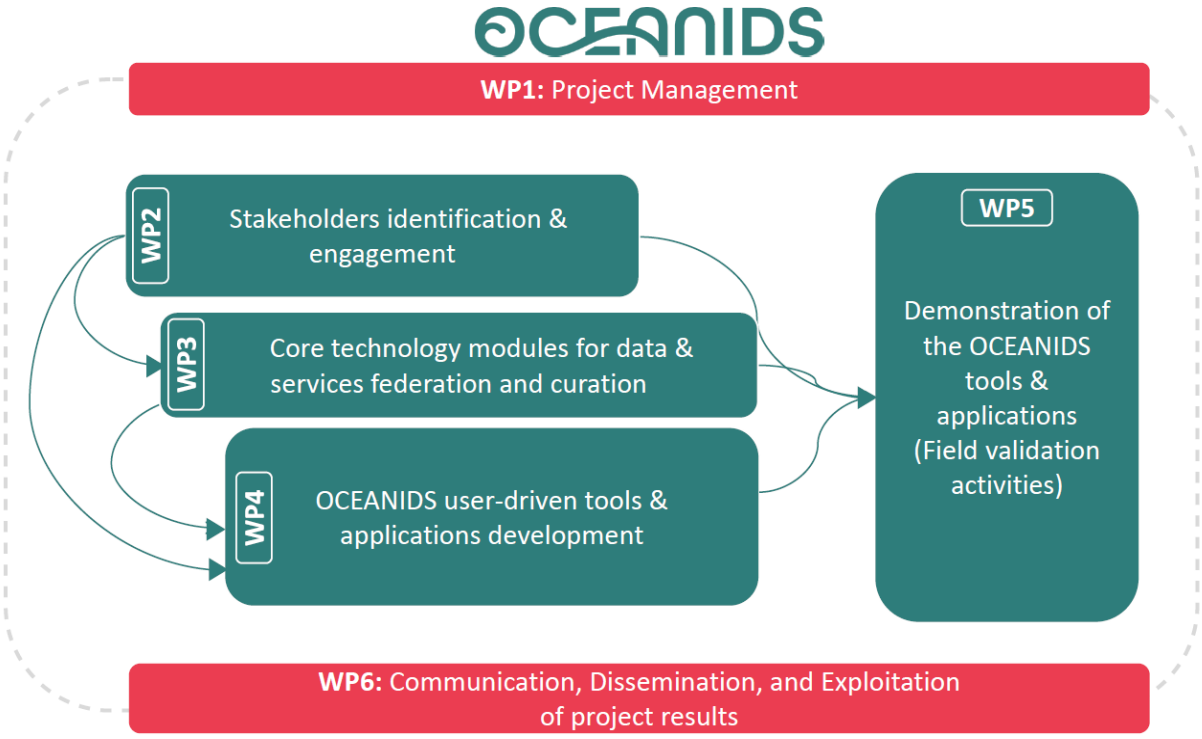

Figure 1. OCEANID'S WPs structure workflow

2 The OCEANIDS Data Cubes Framework Architecture and Comparison with the Literature Data Cubes

A **Data Cube (DC)**[11], [12] is defined as a multidimensional array containing all the necessary information (i.e., data, metadata, geolocation, etc.) describing a phenomenon. To better understand a basic Earth Observation DC framework, let us denote it as a 2D array. $B_i(x, y)$A Spectral band (i.e., image) of a satellite product or a representation of a climate/meteorological parameter. Thus, each coordinate set (x, y) corresponds to a radiometric representation value for a specific spectral channel or climate/meteorological parameter.

In **remote sensing**, a satellite retrieves data on several wavelengths, which means that it generates several images for different wavelengths of the spectrum (i.e., Coastal Aerosol, Blue, Green, Red, Near Infrared, etc.). Similarly, it is possible to produce several raster datasets of climate/meteorological parameters over a specific area of interest. The combination of these images can generate derivative products for monitoring one or more phenomena.

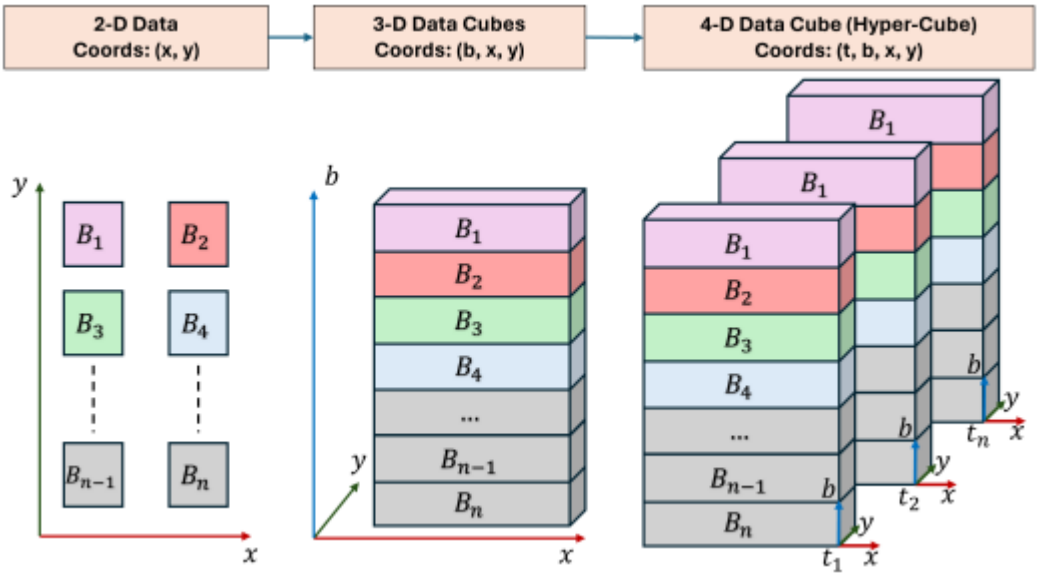

Figure 2. An example of a Data Cube's dimension expanding

Usually, raw data are captured or produced in different spatial resolutions (i.e., 10 m/px, 15 m/px, 30 m/px, 60 m/px, 250 m/px, 0.5 km/px, 1.1 km/px, etc.), thus any combinations and/or calculations cannot be achieved in the original state of data. This issue is addressed by expanding the DC's dimension through processing the raw data to match both spatial resolution and coordinates. Let $DC(b, x, y) = [B_1(x, y), B_2(x, y), \dots, B_N(x, y)]$ denote a 3D DC, where each layer B_i *(x, y)* represents an image at a common spatial resolution and coordinate reference system (CRS).

Finally, the dynamic monitoring of a phenomenon introduces the parameter of time (t). Thus, for effective monitoring of a periodic phenomenon (i.e., temperature, humidity, sea level, waves, wind speed, etc.) over an area and for detecting abnormalities, it is necessary to generate a 4D DC (Hypercube). A Hypercube is defined as a 4D DC containing *N* 3D-DC layers

of different time periods(i.e., before, in between and after an event or activity) and can be mathematically denoted by the equation as follows: $HDC_i(t,b,x,y) = [DC_{t1}(b,x,y), DC_{t2}(b,x,y), \dots, DC_{tN}(b,x,y)]$. **Figure 2** illustrates the expansion of the dimensions of a DC as described in the previous paragraphs.

2.1 Existing Earth Observation Data Cubes Implementations

As previously indicated, **a DC is a multidimensional array or a data structure** that allows the efficient analysis, representation, and visualization of big data structures along multiple dimensions. A DC framework is mostly used for applications regarding big data storage and online analytical processing (OLAP)[13] based on complex queries[14] and analysis[15]. Major functionalities of a DC framework are: (a) multidimensional representation[16]; (b) cube structure for big data visualizations[17]; (c) data aggregation [18]; (d) fast query performance[19]; (e) OLAP operations[20]; and (d) smart big data applications[21].

The current existing DCs' implementations are emphasized in organizing the data on multiple dimensions[22], like time, geography, product, or customer. Each dimension represents a different aspect of the data. Thus, a **DC's structure** is often visualized as a cube with multiple dimensions. Each cell in the cube's representation is a unique combination of dimensional values. For instance, in a remote sensing DC, an indicative combination can be the vector $(time\ x\ spectral\ bands\ x\ geografical\ coordinates)$. Moreover, in other examples of DCs, like climatic and geographical DCs, the data can be aggregated using traditional aggregation functions like mean, count, average, minimum, and maximum (i.e., mean temperature, maximum wind speed, average humidity, etc.).

At this point, it is important to note that numerical values alone are not enough to describe a complex natural phenomenon. Thus, the strong characteristic of the DCs' representations is the **inclusion of metadata information**, which describes the numerical values of the data[23]. Such information includes the metric system of the data, the origin of the data, geo-spatial information, climate/meteorological conditions during data collection, etc. This information can be used to **achieve fast query performance**, which is one of the advantages of using DCs, especially when dealing with large volumes of data (i.e., addressing big data storage performance issues).

Several DC implementations have been proposed in the past years. An indicative example is the work of Ferreira et al.[24], where they proposed an effective way for generating **EODCs** over Brazil. They additionally exploited the benefits of the Open Data Cubes' platform[1], contributing by conducting analysis-ready data and multidimensional DCs from remote sensing images to effectively map the land use and land cover based on employing remote sensing imagery time series analysis and machine learning techniques.

The **Australian Geoscience DC** is one of the first DC implementations, proposed by Lewis et al.[25] and manages the challenges of big data, such as the storage volume, velocity, and polymorphism or variety, limiting the earth observation data usefulness. Some of the

[1] https://www.opendatacube.org/

applications, where the Australian Geoscience DC has been applied are: (a) water observations; (b) coastal erosion; (c) agriculture monitoring; (d) forest cover changes; and (e) biodiversity.

In the work of Poussin et al.[26] the advantages and limitations of the **Earth Observation Swiss DCs** are exploited by monitoring the snow cover change in Gran Paradiso National Park, Alps. EO Swiss DCs' architecture is based on the Open Data Cubes software[27], which is a geospatial data management and analysis software based on open-source technologies for processing remote sensing data by providing a framework for accessing, storing, managing, and analyzing grid-aligned satellite EO data collections in huge quantities.

Other works utilizing the **EO Swiss DCs** implementations are proposed by Giuliani et al.[18], [28]. Within the first work, they propose a methodology for generating accurate and consistent land degradation products based on remote sensing imagery datasets. They use a generated DC and several sun-indicators for assessing land productivity and cover, as well as soil organic carbon changes for evaluating land degradation. The second work proposes the use of an on-demand DC, implemented as a script-based tool, to automate the generation of data cubes according to user-defined requirements. Such requirements can be the polygon of the area of interest, a time period, the type of sensor, or the satellite product family. Their implementation has been successfully applied to two regions (Bolivia and the Democratic Republic of Congo) for environmental monitoring.

Finally, Temenos et al.[29] propose **a context-aware adaptive DC framework**, which utilizes EO data for environmental monitoring for mitigating the climate change effects. Their proposed methodology combines the DCs' formation with the calculation of remote sensing operations, including deep and machine learning algorithms for data classification and harmonization. Thus, the outcome is a context-aware adaptive framework, which successfully allows the environmental monitoring and climate change effects based on user-predetermined preferences.

2.2 The OCEANIDS Data Cubes framework

Considering the current literature, the OCEANIDS project develops a DC framework for monitoring the oceanic and coastal regions. To be more precise, the **ODCs** provide data harmonization and homogenization of huge amounts of data provided by several different sources. These data can be EO remote sensing imagery (i.e., Landsat-8, Sentinel-2) or climate/meteorological time-series forecasting (i.e., EUROCORDEX data).

Thus, the main objective of the ODC framework is to provide harmonization and homogenization between several available EO products, including both remote sensing imagery and climate/meteorological products. In addition, non-EO data has been used for providing extra information, such as the boundary of the area of interest. **Figure 3** illustrates the ODCs' architecture and framework workflow.

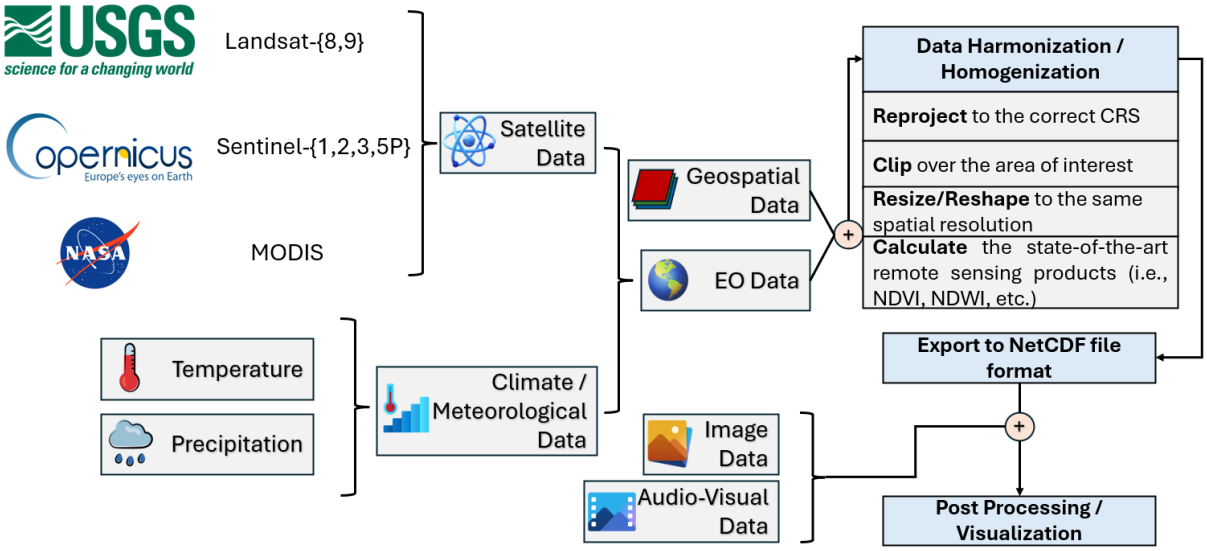

Figure 3. The OCEANIDS Data Cubes' architecture and framework workflow

The first step of the framework is to **collect and store all relevant raw data**. The data can be satellite imagery, such as Landsat-8/Landsat-9 missions provided by USGS[30], Sentinel-1/ Sentinel-2/Sentinel-3/Sentinel-5P provided by Copernicus services[31], and MODIS data from NASA[32]. The climate and meteorological data include EUROCORDEX time-series forecasts[33] and other atmospheric data from the Copernicus HUB[34]. The supported non-EO data are polygon shapefiles (SHP) geometries, which indicate the areas of interest. All this data is fed to the framework for generating an ODC product.

The **Data Harmonization/Homogenization** step is a core component of the ODC framework. Its implementation depends on the characteristics of the raw data and may, in some cases, differ from the version illustrated in **Figure 3**. For example, climate/meteorological data requires only the reprojection and clipping steps. The EO data are handled differently depending on their original format (i.e., Sentinel-2 and Landsat missions follow the full processing workflow as illustrated in **Figure 3**, while Sentinel-3 and Sentinel-5P data require only reprojection and clipping).

Another important feature of the framework is that the clipping step varies depending on the data type. For example, the EO data are clipped using a shapefile geometry that bounds the area of interest, while the climate/meteorological data are clipped as a NxN (i.e., 2x2, 3x3, 4x4, etc.) grid. Similarly, the reprojection and resize steps are applied based on the characteristics of the raw data. Additional details about these approaches are provided in the following sections.

The **output product of the Data Harmonization/Homogenization step** is a NetCDF file format, following a common and strict template to ensure interoperability, consistency, and compatibility with downstream processes. The template includes the following core components:

1. Dimensions

- `time`:
  Represents the temporal dimension of the dataset.
  - **Type:** Unlimited or fixed
  - **Units:** `days since YYYY-MM-DD` or `hours since YYYY-MM-DD HH:MM:SS`
  - **Example:** `time = 12 ;`
- `lat (latitude):`
  Geographic latitude values.
  - **Type**: 1D float array
  - **Units**: degrees north
  - **Resolution**: Varies by dataset (e.g., 0.01°, 0.25°)
- `lon (longitude):`
  Geographic longitude values.
  - **Type**: 1D float array
  - **Units**: degrees east
  - **Resolution**: Matches lat
- `band` or `variable` (optional):
  Spectral or thematic layer index (e.g., NDVI, RGB, temperature)
  - **Type**: Integer or string dimension

2. Variables

Each variable stores actual data and is defined along one or more dimensions.

- `<product_variable>`(e.g., `NDVI`, `Temperature`, `RGB_red`) :
  The main data variable(s) from EO or climate datasets.
  - **Dimensions:** `[time, band?, lat, lon]`
  - **Units:** Depends on the variable (e.g., `Kelvin`, `unitless`, %)
  - **Missing values:** Defined using `_FillValue` attribute
  - **Compression:** `deflate_level = 4-9` (optional)
- `lat` / `lon`:
  Arrays storing latitude and longitude values for each grid point.
  - **Units:** as above
- `time`:

  Time values mapped to real calendar dates using a reference format.

3. Global Attributes

Descriptive metadata about the dataset:

Attribute	Description
`title`	Descriptive title of the dataset (e.g., "Monthly NDVI for Crete")
`summary`	Brief overview of the dataset purpose and contents
`source`	Source dataset (e.g., "Sentinel-2 Level-2A")
`institution`	Producing institution or project (e.g., "OCEANIDS Project")
`history`	Processing steps with timestamps
`references`	Related publications or DOIs
`Conventions`	"CF-1.8" (Climate and Forecast metadata conventions)
`creator_name`	Contact person or group
`geospatial_bounds`	Extent of the dataset in WKT or bounding box format

4. Variable Attributes

Each data variable should include:

- `long_name:` Human-readable name (e.g., "Normalized Difference Vegetation Index")
- `units:` Units of measurement
- `_FillValue:` Value used to denote missing or invalid data (e.g., `-9999`)
- `valid_range:` Expected value range (e.g., `[0.0, 1.0]` for NDVI)
- `coordinates:` Indicates associated coordinates (e.g., "`lat lon time`")

The NetCDF file format was selected because it is capable of storing several data types along with metadata information, and it is widely supported by several software (i.e., QGIS[2], ArcGIS[3], GDAL[4], etc.) and services (i.e., GeoServer[5]). This means that the ODCs are standardized products, which makes their visualization and post-processing feasible and easier with the current market software.

Finally, **post-processing activities** can be applied to the generated products. Several examples of such activities (but not restricted to) are the following: (a) thematic mapping for monitoring climate phenomena; (b) time series analysis; (c) coastline changes monitoring; (d) port activity monitoring; (e) early warning systems; (f) decision support systems; and (g) damage management (i.e., prediction, size/cost estimation, etc.).

2.2.1 OCEANIDS Climate/Meteorological Data Cubes Description

The Climate/Meteorological data, which are used in the OCEANIDS project, include several climate parameters from the **CORDEX** (Coordinated Regional Climate Downscaling Experiment) datasets, as presented in **Table 2**. CORDEX is a global initiative led by the WCRP (World Climate Research Programme) that provides high-resolution regional climate projections through standardized downscaling of global climate model outputs – these datasets are usually shared in NetCDF file formats.

The CORDEX experiment divides the world into 14 domains, where different research groups run **RCMs (Regional Climate Models)** or apply statistical methods to generate locally detailed

[2] https://qgis.org/
[3] https://www.arcgis.com/index.html
[4] https://gdal.org/en/stable/
[5] https://geoserver.org/

climate and meteorological data. Thus, these datasets bridge the gap between coarse-scale global projections and the fine-scale information needed for local impact assessments. CORDEX provides multi-model climate simulations based on both historical and future emission scenarios (i.e., RCPs such as RCP4.5, RCP8.5, and SSPs) at spatial resolutions of 50km, 25km, and 11.5km. These datasets cover variables such as temperature, precipitation, humidity, and wind with temporal resolutions ranging from daily to 6-hour intervals.

The main scope of CORDEX data is to provide regional climate projections that can be used in different applications. Such applications can be the following: (a) refinement of downscaling techniques; (b) the production of consistent climate projections across regions; (c) support decision-making, and others. These applications align with the objectives of the OCEANIDS project, making CORDEX datasets suitable for modeling climate extremes and geographic influences (i.e., coastal and maritime/port regions monitoring), which global models are unable to resolve accurately.

In addition, CORDEX datasets play a significant role in supporting climate adaptation and mitigation planning. They can be used in diverse applications like assessing future water resources, designing resilient infrastructures (i.e., in coastal regions), and estimating climate-related risks. The regional projections under different emission scenarios help in supporting the decision-making of local authorities by predicting the climate impact of their decisions. **CORDEX outputs** have been widely adopted in national climate plans, academic research, and international assessments, making them a cornerstone of resources for translating global climate science into regional actionable information[35].

In the OCEANIDS project, CORDEX data are used for various applications related to climate monitoring in coastal regions, emphasizing the port pilot regions of the project. The raw dataset is composed of several climate projections, including the **following parameters**: (a) **clt [%]**: duration of sunshine; (b) **hurs [%]**: near-surface relative humidity; (c) **taxman [K]**: daily maximum near-surface air temperature; (d) **taxmin [K]**: daily minimum near-surface air temperature; (e) **pr [$\frac{kg\ x\ m^2}{s}$]**: precipitation; (f) **sfcWind [$\frac{m}{s}$]**: near surface wind speed; (g) **uas [$\frac{m}{s}$]**: eastwards near-surface wind; and (h) **vas [$\frac{m}{s}$]:** northwards near-surface wind. Table 2 summarizes the raw CORDEX datasets used for the generation of OCEANIDS Data Cubes in the project.

Table 2. CORDEX dataset for the OCEANIDS project

CORDEX Type	Projection Name	Time Window	Start Date – End Date	Dataset Step in Years	Parameters
hist	cnrm_cerfacs_cm5-cnrm_aladin63	6hours	1970-2005	1	uas, vas
hist	cnrm_cerfacs_cm5-cnrm_aladin63	daily	1971-2001	5	clt, hurs, taxmax, taxmin, pr, sfcWind
hist	cnrm_cerfacs_cm5-knmi_racmo22e	6hours	1970-2005	1	uas, vas

hist	cnrm_cerfacs_cm5-knmi_racmo22e	daily	1971-2001	5	clt, hurs, taxmax, taxmin, pr, sfcWind
hist	mohc_hadgem2_es-dmi_hirham5	6hours	1970-2005	1	uas, vas
hist	mohc_hadgem2_es-dmi_hirham5	daily	1971-2001	5	clt, hurs, taxmax, taxmin, pr, sfcWind
hist	mohc_hadgem2_es-knmi_racmo22e	6hours	1970-2005	1	uas, vas
hist	mohc_hadgem2_es-knmi_racmo22e	daily	1971-2001	5	clt, hurs, taxmax, taxmin, pr, sfcWind
hist	mohc_hadgem2_es-smhi_rca4	6hours	1970-2005	1	uas, vas
hist	mohc_hadgem2_es-smhi_rca4	daily	1971-2001	5	clt, hurs, taxmax, taxmin, pr, sfcWind
hist	ncc_noresm1_m-dmi_hirham5	6hours	1970-2005	1	uas, vas
hist	ncc_noresm1_m-dmi_hirham5	daily	1971-2001	5	clt, hurs, taxmax, taxmin, pr, sfcWind
hist	ncc_noresm1_m-smhi_rca4	6hours	1970-2005	1	uas, vas
hist	ncc_noresm1_m-smhi_rca4	daily	1971-2001	5	clt, hurs, taxmax, taxmin, pr, sfcWind
rcp45	cnrm_cerfacs_cm5-cnrm_aladin63	6hours	2006-2100	1	uas, vas
rcp45	cnrm_cerfacs_cm5-cnrm_aladin63	daily	2006-2096	5	clt, hurs, taxmax, taxmin, pr, sfcWind
rcp45	cnrm_cerfacs_cm5-knmi_racmo22e	6hours	2006-2100	1	uas, vas
rcp45	cnrm_cerfacs_cm5-knmi_racmo22e	daily	2006-2096	5	clt, hurs, taxmax, taxmin, pr, sfcWind
rcp45	mohc_hadgem2_es-dmi_hirham5	6hours	2006-2100	1	uas, vas
rcp45	mohc_hadgem2_es-dmi_hirham5	daily	2006-2096	5	clt, hurs, taxmax, taxmin, pr, sfcWind
rcp45	mohc_hadgem2_es-knmi_racmo22e	6hours	2006-2100	1	uas, vas
rcp45	mohc_hadgem2_es-knmi_racmo22e	daily	2006-2096	5	clt, hurs, taxmax, taxmin, pr, sfcWind
rcp45	mohc_hadgem2_es-smhi_rca4	6hours	2006-2100	1	uas, vas

rcp45	mohc_hadgem2_es-smhi_rca4	daily	2006-2096	5	clt, hurs, taxmax, taxmin, pr, sfcWind
rcp45	ncc_noresm1_m-dmi_hirham5	6hours	2006-2100	1	uas, vas
rcp45	ncc_noresm1_m-dmi_hirham5	daily	2006-2096	5	clt, hurs, taxmax, taxmin, pr, sfcWind
rcp45	ncc_noresm1_m-smhi_rca4	6hours	2006-2100	1	uas, vas
rcp45	ncc_noresm1_m-smhi_rca4	daily	2006-2096	5	clt, hurs, taxmax, taxmin, pr, sfcWind
rcp85	cnrm_cerfacs_cm5-cnrm_aladin63	6hours	2006-2100	1	uas, vas
rcp85	cnrm_cerfacs_cm5-cnrm_aladin63	daily	2006-2096	5	clt, hurs, taxmax, taxmin, pr, sfcWind
rcp85	cnrm_cerfacs_cm5-knmi_racmo22e	6hours	2006-2100	1	uas, vas
rcp85	cnrm_cerfacs_cm5-knmi_racmo22e	daily	2006-2096	5	clt, hurs, taxmax, taxmin, pr, sfcWind
rcp85	mohc_hadgem2_es-dmi_hirham5	6hours	2006-2100	1	uas, vas
rcp85	mohc_hadgem2_es-dmi_hirham5	daily	2006-2096	5	clt, hurs, taxmax, taxmin, pr, sfcWind
rcp85	mohc_hadgem2_es-knmi_racmo22e	6hours	2006-2100	1	uas, vas
rcp85	mohc_hadgem2_es-knmi_racmo22e	daily	2006-2096	5	clt, hurs, taxmax, taxmin, pr, sfcWind
rcp85	mohc_hadgem2_es-smhi_rca4	6hours	2006-2100	1	uas, vas
rcp85	mohc_hadgem2_es-smhi_rca4	daily	2006-2096	5	clt, hurs, taxmax, taxmin, pr, sfcWind
rcp85	ncc_noresm1_m-dmi_hirham5	6hours	2006-2100	1	uas, vas
rcp85	ncc_noresm1_m-dmi_hirham5	daily	2006-2096	5	clt, hurs, taxmax, taxmin, pr, sfcWind
rcp85	ncc_noresm1_m-smhi_rca4	6hours	2006-2100	1	uas, vas
rcp85	ncc_noresm1_m-smhi_rca4	daily	2006-2096	5	clt, hurs, taxmax, taxmin, pr, sfcWind

The raw CORDEX data are distributed as **gridded images**, with a resolution of $0.44^o\ x\ 0.44^o$ using a rotated pole coordinate system. In reality, the model operates over an equatorial

domain with a quasi-uniform resolution of approximately. $50km$. Thus, the ODC framework performs the necessary technical analysis based on the CORDEX domain information to transform the rotated coordinates to correspond to WGS84 (EPSG:4326) latitude and longitude.

Before describing the calculations, it is necessary to define the following **parameters** as presented in the CORDEX domain documentation[36]. These parameters represent specific coordinates (Longitude, Latitude) of characteristic image points. To be more precise, these points are the following: (a) Top Left Corner (TLC); (b) Centre Northern Boundary (CNB); (c) Top Right Corner (TRC); (d) Center Western Boundary (CWB); (e) Centre Point of the Domain (CPD); (f) Center Eastern Boundary (CEB); (g) Bottom Left Corner (BLC); (h) Center Southern Boundary (CSB); and (i) Bottom Right Corner (BRC). **Equations 3.1–3.13** presents a visual representation of the CORDEX rotated coordinates parameters.

Equations 3.1-3.13 provide the necessary background to transform coordinates from WGS84 to Rotated Coordinates and vice versa.

$$\theta = \frac{\pi \; x \; lat_{RotPole}}{180} \tag{3.1}$$

$$\varphi = \frac{\pi \; x \; lon_{RotPole}}{180} \tag{3.2}$$

$$X_{WGS84} = \cos(lon_{WGS84}) \; x \; cos(lat_{WGS84}) \rightarrow X_{Rot} = \cos(lon_{Rot}) \; x \; cos(lat_{Rot}) \tag{3.3}$$

$$Y_{WGS84} = \sin(lon_{WGS84}) \; x \; cos(lat_{WGS84}) \rightarrow Y_{Rot} = \sin(lon_{Rot}) \; x \; cos(lat_{Rot}) \tag{3.4}$$

$$Z_{WGS84} = \sin(lat_{WGS84}) \rightarrow Z_{Rot} = sin(lat_{Rot}) \tag{3.5}$$

$$X_{WGS84 \rightarrow Rot} = \cos(\theta) * \cos(\varphi) * X_{WGS84} + \cos(\theta) * \sin(\varphi) * Y_{WGS84} + \sin(\varphi) * Z_{WGS84} \tag{3.6}$$

$$Y_{WGS84 \rightarrow Rot} = -\sin(\varphi) * X_{WGS84} + \cos(\varphi) * Y_{WGS84} \tag{3.7}$$

$$Z_{WGS84 \rightarrow Rot} = -\sin(\theta) * \cos(\varphi) * X_{WGS84} - \sin(\theta) * \sin(\varphi) * Y_{WGS84} + \cos(\theta) * Z_{WGS84} \tag{3.8}$$

$$X_{Rot \rightarrow WGS84} = \cos(\theta) * \cos(\varphi) * X_{Rot} + \sin(\varphi) * Y_{Rot} + \sin(\theta) * \sin(\varphi) * Z_{Rot} \tag{3.9}$$

$$Y_{Rot \rightarrow WGS84} = -\cos(\theta) * \sin(\varphi) * X_{Rot} + \cos(\varphi) * Y_{Rot} - \sin(\theta) * \sin(\varphi) * Z_{Rot} \tag{3.10}$$

$$Z_{Rot \rightarrow WGS84} = -\sin(\theta) * X_{Rot} + \cos(\theta) * Z_{Rot} \tag{3.11}$$

$$lon_{i \rightarrow j} = atan2(X_{i \rightarrow j}, Y_{i \rightarrow j}) \tag{3.12}$$

$$lat_{i \rightarrow j} = \text{asin}(Z_{i \rightarrow j}) \tag{3.13}$$

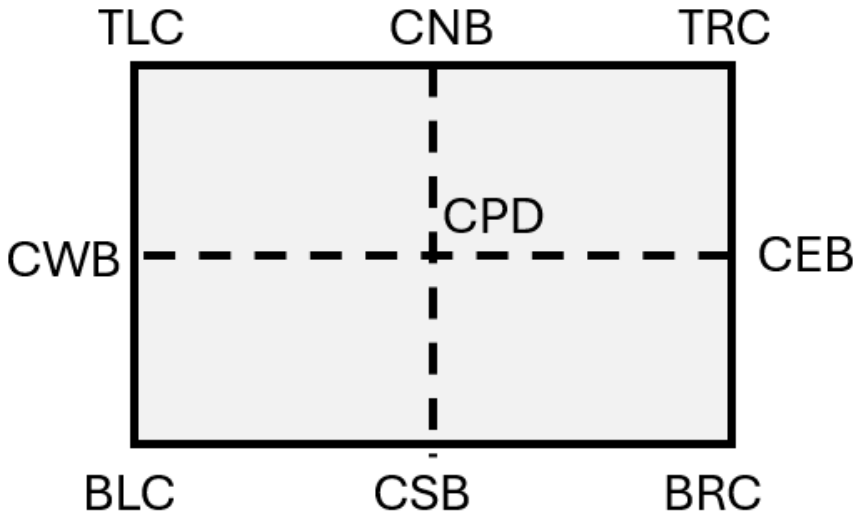

Figure 4. Parameters of the CORDEX rotated coordinates

Thus, by knowing the **transformation parameters**, it is easy to retrieve the necessary information from the CORDEX data. In the case of OCEANIDS Data Cubes, it is a NxN (i.e., $2x2$) grid surrounding the central coordinate of each area of interest. The parameters of the EURO CORDEX domain (**Figure 4-5**), which is used in the OCEANIDS project, are presented in **Table 3.**

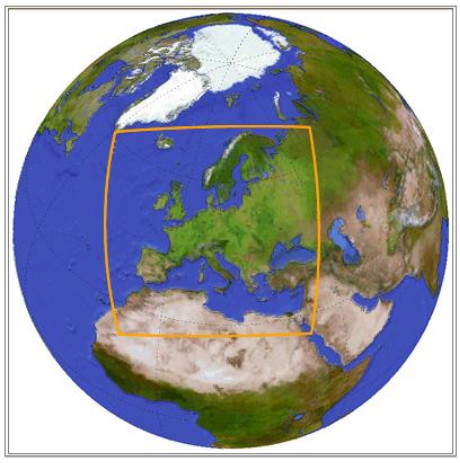

Figure 5. EURO CORDEX Domain[36]

Table 3. EURO CORDEX Parameters[36]

Parameter	Values
RotPole (lon_{Rot}, lat_{Rot})	(198.0, 39.25)
TCL (lon_{Rot}, lat_{Rot})	(331.79, 21.67)

N_x	106
N_y	103
TLC (lon_{WGS84}, lat_{WGS84})	(315.86, 60.21)
CNB (lon_{WGS84}, lat_{WGS84})	(1.92, 71.84)
TRC (lon_{WGS84}, lat_{WGS84})	(64.40, 66.65)
CWB (lon_{WGS84}, lat_{WGS84})	(338.23, 42.36)
CPD (lon_{WGS84}, lat_{WGS84})	(9.75, 49.68)
CED (lon_{WGS84}, lat_{WGS84})	(44.77, 46.72)
BLC (lon_{WGS84}, lat_{WGS84})	(350.01, 22.20)
CSB (lon_{WGS84}, lat_{WGS84})	(12.48, 27.34)
BRC (lon_{WGS84}, lat_{WGS84})	(36.30, 25.36)

2.2.2 OCEANIDS Earth Observation Data Cubes Description

The OCEANIDS project uses several EO datasets to achieve its various tasks and activities. The data are provided by **different sources** in different resolutions, capturing sensors, and formats. Mainly, this project handles Landsat (source: USGS – Earth Explorer[30]) and Sentinel (source: Copernicus Data Space[31]) missions. In addition, the MODIS mission serves as a low-resolution alternative for atmospheric and ocean monitoring. **Table 4** summarizes the EO data sources used in the OCEANIDS project.

Table 4. EO Data Sources

EO Mission	Description	Data that can be used in the project	Data Source
Sentinel-1[37]	Sentinel-1 mission consists of two polar-orbiting satellites, operating day and night for both land and ocean monitoring. The satellites are equipped with C-band SAR sensors that enable image capturing regardless of weather conditions. The mission has a 12-day cycle.	C-band SAR with center frequency $5.405\ GHz$. Polarization: VV+VH; HH+HV; HH; VV. Resolutions: (a) *Strip map mode* of $80km$ swath and $5m\ x\ 5m$ spatial resolution. (b) *Interferometric Wide Swath* of $250m$ swath and $5m\ x\ 20m$ spatial resolution. (c) *Extra-Wide Swath Mode* of $400km$ swath and $20m\ x\ 40m$ spatial resolution.	Copernicus Data Space

		(d) *Wave Mode* of $20km\ x\ 20km$ or $5m\ x\ 5m$ spatial resolutions.	
Sentinel-2[38]	Sentinel-2 mission consists of three polar-orbiting satellites that provide high-resolution optical imagery aiming at land monitoring. Vegetation, soil, and coastal areas monitoring are some of this mission's objectives. The mission has a 10-day cycle per satellite and a 5-day revisit time considering both satellites.	**B01** – Coastal Aerosol (Spatial Resolution $60m$) **B02** – Blue (Spatial Resolution $10m$) **B03** – Green (Spatial Resolution $10m$) **B04** – Red (Spatial Resolution $10m$) **B05** – Vegetation Red Edge (Spatial Resolution $20m$) **B06** – Vegetation Red Edge (Spatial Resolution $20m$) **B07** – Vegetation Red Edge (Spatial Resolution $20m$) **B08** – Near Infrared (Spatial Resolution $10m$) **B08A** – Vegetation Red Edge / Narrow Near Infrared (Spatial Resolution $20m$) **B09** – Water Vapor (Spatial Resolution $60m$) **B10** – SWIR-CIRRUS (Spatial Resolution $60m$) **B11** – SWIR (Spatial Resolution $20m$) **B12** – SWIR (Spatial Resolution $20m$)	Copernicus Data Space
Sentinel-3[39]	Sentinel-3 mission consists of three satellites. This mission's primary instrument is a radar altimeter. The polar-orbiting satellites carry several instruments, including optical imagers. The main objectives are: (a) Marine observation; (b) Sea-surface topography; (c) Sea and land surface temperature; and (d) Ocean and Land color. The orbital cycle is 27 days.	From the three processing modes of the OLCI processor (Earth Observation-EO, Radiometric Calibration-RC, and Spectral Calibration-SC) and two available resolutions (Full-FR and Reduced-RR), four different products are obtained. <u>Level 1 Products:</u> OL_1_EFR: Output during EO processing mode for FR. OL_1_ERR: Output during EO processing mode for RR. OL_1_RAC: Output during RC mode. OL_1_SPC: Output during SC mode. <u>Level 2 Products:</u> Land Reduced Products (OL_2_LRR) or Full (OL_2_LFR) Resolution products are outputs from the OLCI-Level-2 processor. They contain land and atmospheric geophysical products at FR	Copernicus Data Space

		and RR. The spatial resolution of OLCI products is approximately $300m$ at FR and approximately $1.2km$ at RR. The SLTR products are divided into six main categories: Level 1B RBT (Radiance and Brightness Temperature) Level 2 WCT (Water Combined Temperature) Level 2 LST (Land Surface Temperature) Level 2 FRP (Fire Radiative Power) Level 2 AOD (Global Aerosol Optical Depth) The spatial resolution for the SLSTR product is $50m$ for solar reflectance bands (S1-S6) and $1km$ resolution for Thermal Infrared Bands (S7-S9 and F1-F2).	
Sentinel-5P[40]	Sentinel-5P is a precursor satellite mission aiming at filling in the data gap by providing data continuity between the retirement of the Envisat satellite and NASA's Aura mission, along with the launch of Sentinel-5. Thus, this mission performs atmospheric measurements with high spatiotemporal resolution relating to air quality, climate forcing, ozone, and UV radiation.	There are three types of processing required: (a) near real-time – NRT; (b) offline – OFF; and Reprocessing. Sentinel-5P collects data referring to: (a) Ozone (O_3); (b) Sulphur Dioxide (SO_2); (c) Nitrogen Dioxide (NO_2); (d) Carbon Monoxide (CO); (e) Formaldehyde (H_2CO); and (f) Vertical profiles of Ozone Cloud and Aerosol.	Copernicus Data Space
Landsat-1/5 MSS[41]	Landsat-1/5 mission is equipped with the Multispectral Scanner (MSS), which is a pioneering sensor. Its products are mostly used for long-term, systematic EO applications like agriculture, forestry, geology, and land-use monitoring and planning.	**B01** – Green (Spatial Resolution $60m$) **B02** – Red (Spatial Resolution $60m$) **B03** – Ultra Red (Spatial Resolution $60m$) **B04** – Near Infrared (Spatial Resolution $60m$)	USGS Earth Explorer
Landsat-4/5 TM[42]	Landsat-4/5 mission is equipped with the Thematic Mapper (TM) sensor, which enables detailed and accurate analysis of land surface conditions, like vegetation health, soil moisture, urban	**B01** – Blue (Spatial Resolution $30m$) **B02** – Green (Spatial Resolution $30m$) **B03** – Red (Spatial Resolution $30m$) **B04** – Near Infrared (Spatial Resolution $30m$)	USGS Earth Explorer

	development, and coastal monitoring.	**B05** – SWIR (Spatial Resolution $30m$) **B06** – TIRS (Spatial Resolution $120m$) **B07** – SWIR (Spatial Resolution $30m$) **B08** – Panchromatic (Spatial Resolution $15m$)	
Landsat-7 ETM+[43]	Landsat-7 mission carries the Enhanced Thematic Mapper Plus (ETM+), which is an advanced sensor building on the capabilities of TM. This mission can be used for a precise analysis of agriculture, forest, and water resource monitoring, urban planning, and disaster assessment.	**B01** – Blue (Spatial Resolution $30m$) **B02** – Green (Spatial Resolution $30m$) **B03** – Red (Spatial Resolution $30m$) **B04** – Near Infrared (Spatial Resolution $30m$) **B05** – SWIR (Spatial Resolution $30m$) **B06** – VCID-1 (Spatial Resolution $30m$) **B06** – VCID-2 (Spatial Resolution $30m$) **B07** – SWIR (Spatial Resolution $30m$) **B08** – Panchromatic (Spatial Resolution $15m$)	USGS Earth Explorer
Landsat-8/9 OLI-TIRS[44]	Landsat-8/9 mission carries two types of instruments: (a) Operational Land Imager (OLI) and (b) Thermal Infrared Sensor (TIRS). This mission is currently used for critical applications, including agricultural and coastal monitoring, water resource management, land use and land cover mapping, wildfire tracking, and urban heat island effect.	**B01** – Coastal Aerosol (Spatial Resolution $30m$) **B02** – Blue (Spatial Resolution $30m$) **B03** – Green (Spatial Resolution $30m$) **B04** – Red (Spatial Resolution $30m$) **B05** – Near Infrared (Spatial Resolution $30m$) **B06** – SWIR (Spatial Resolution $30m$) **B07** – SWIR (Spatial Resolution $30m$) **B08** – Panchromatic (Spatial Resolution $30m$) **B09** – CIRRUS (Spatial Resolution $30m$) **B10** – TIRS (Spatial Resolution $100m$) **B11** – TIRS (Spatial Resolution $100m$)	USGS Earth Explorer
MODIS[45]	MODIS is a key instrument aboard the Terra and Aqua satellites, which are viewing the Earth's surface every 1-2 days, acquiring data in 36 spectral bands or groups of wavelengths. Spatial Resolutions:	**B01-B07** – Land / Cloud / Aerosols **B08-B16** – Ocean Colour / Phytoplankton / Biogeochemistry **B17-B19** – Atmospheric Water Vapor **B20-B23** – Surface / Cloud Temperature **B24-B25** – Atmospheric Temperature **B26-B28** – Cirrus Clouds Water Vapor	MODIS NASA Website USGS GLOVIS USGS Earth Explorer

	(a) $250m$ for B01-B02; (b) $500m$ for B03-B07; (c) $1km$ for B08-B36.	**B29** – Cloud Properties **B30** – Ozone **B31-B32** – Surface / Cloud Temperature **B33-B36** – Cloud Top Altitude	

While all the data included in **Table 4** can be used in different OCEANIDS applications, the ODC framework primarily focuses on handling **Sentinel-2** and **all Landsat missions**. This is due to two main reasons: **(a)** These datasets are based on optical bands and they can be used together to generate similar products for similar applications; **(b)** Sentinel-1, Sentinel-3 and Sentinel-5P products are downloaded in several and different already ready-to-use architectures and further processing can be handled using ESA's Sentinel Toolboxes[46].

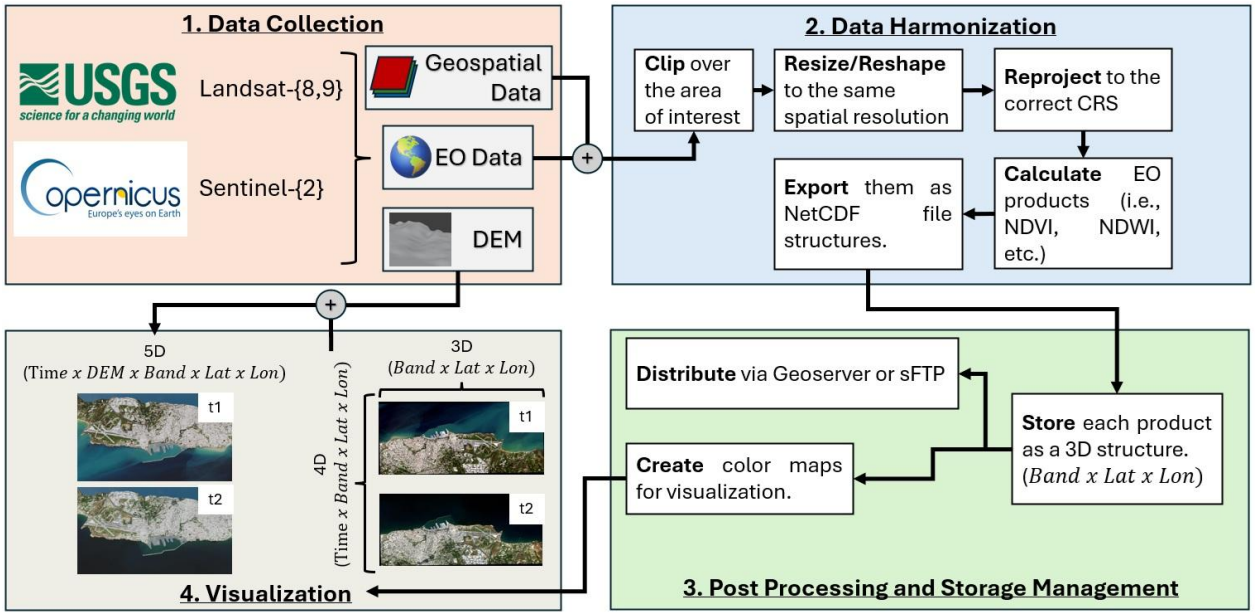

Figure 6. The workflow of ODC EO Services

Figure 6 illustrates the comprehensive workflow of ODC EO services as developed for the needs of the OCEANIDS project. The workflow is suitable for generating ready-to-use products based on EO data for monitoring coastal regions through a systematic four-stage methodology: **(1)** Data Collection; **(2)** Data Harmonization; **(3)** Port-Processing and Storage Management; and **(4)** Visualization.

At this point, it is necessary to mention that the ODC framework is **publicly available on GitLab**[47] as a cross-platform solution compatible with all major operating systems (Windows, Linux, macOS). This framework has been developed using Python, and it can be deployed and executed under a Python Virtual Environment. This implementation enables full reproducibility of the data harmonization pipeline, facilitating validation studies and collaborative development, while the shared codebase allows researchers and end users to replicate processing workflows, verify results, and adapt the framework for specific coastal monitoring applications.

The subsequent paragraphs provide detailed information **on each methodological component**, beginning with the data acquisition phase that incorporates multi-source EO datasets, followed by the harmonization procedures designed to ensure data consistency. The post-processing and storage management stage addresses the critical aspect of data organization and accessibility, while the visualization component enables multidimensional analysis of coastal parameters. This approach facilitates robust temporal monitoring of coastal environments while addressing the challenges inherent in large-scale EO data management.

2.2.2.1 Data Collection

Data Collection is considered the first phase of the workflow and the most important because it has a heavy and immediate impact on the results of the next processes. In this step, several EO and non-EO data were collected from various sources or generated in various ways. For example, **the EO data includes**, but is not limited to: **(a)** Landsat mission (i.e., 1/5 MSS, 4/5 TM, 7 ETM+, 8/9 OLI-TIRS) from USGS; **(b)** Sentinel missions (i.e., Sentinel-1, Sentinel-2, Sentinel-3, Sentinel-5P) from Copernicus Data Space; and **(c)** MODIS mission (i.e., TERRA, AQUA) from NASA.

Non-EO data include geospatial geometries that define an area of interest, seasonal or meteorological data or climate data (see *Section 2.2.1*), height-maps (i.e., Digital Elevation Models – DEMs or Digital Terrain Models – DTMs), and other types of supporting datasets. This data can be provided either as time-series (i.e., climate data) or as standalone products (i.e., DEMs or geospatial shapefile geometries). The latter can be generated using geospatial software or obtained through in-situ measurements.

To maintain methodological consistency, in the OCEANIDS project's Task 3.1, applications use data only from online data sources. In addition, the ODC framework handles mainly Landsat missions and Sentinel-2 missions as mentioned above, as they are more aligned with the end-users' needs, such as ports, policy makers, authorities, and research labs, in general, and for the OCEANIDS project, we are referring to ports and coastal municipalities. Geospatial boundaries are generated early in the project as polygon geometries in shapefile (SHP) format, which subsequently serve as spatial masks for clipping EO raster data during the harmonization phase.

In addition, **DEMs** are incorporated as elevation layers, extending the ODCs' dimensionality through the inclusion of vertical (Z-axis) terrain data. The elevation component enables the creation of advanced 3D thematic mapping applications, enhancing visualization fidelity through realistic terrain representation. As a result, the integration of DEM data is particularly valuable for coastal monitoring applications, where topographic variations substantially influence environmental processes.

2.2.2.2 Data Harmonization

The **Data Harmonization phase** integrates all essential processing steps for generating standardized ODC products. This comprehensive procedure involves: **(a)** spatial clipping to the area of interest boundaries; **(b)** resampling all datasets to uniform spatial resolutions; **(c)** reproject the EO products to a consistent Coordinate Reference System (CRS); **(d)** computing

derived spectral indices and products commonly employed in remote sensing analysis; and **(e)** exporting the final data cubes in NetCDF format, which is a widely accepted standard for multidimensional scientific data storage and exchange. This systematic approach ensures spatial and radiometric consistency across all processed datasets while maintaining compatibility with established geospatial analysis workflows. Additionally, the system has been based on the open library XArray, which is a Python library developed specifically for processing remote sensing data and generating data cube structures.

During the **clipping stage,** the spatial extraction of the RAW EO raster data is performed using the predefined shapefile boundary. This operation serves two critical purposes: **(a)** it significantly reduces data volume when processing small areas of interest for facilitating efficient storage and distribution of final products; and **(b)** it establishes the spatial domain for subsequent processing steps. However, the output size exhibits non-linear growth relative to the dimensions of the area of interest, meaning that in some cases the resulting ODC products can exceed the original file size when the clipping boundary represents large areas.

This size inflation occurs because the harmonization process must resample all input radiometric bands, which are typically provided at varying spatial resolutions, to a common target resolution (generally the highest available resolution of the RAW product – i.e., $10m/px$ for Sentinel-2 products or $15m/px$ for Landsat-8/9 products). Consequently, lower-resolution bands undergo substantial up-sampling during this standardization process, resulting in increased storage requirements for the final harmonized product.

The **resampling process** is succeeded by reprojecting the data to the user-defined CRS. By default, the system employs EPSG:4326 (World Geodetic System 1984 – WGS84), which represents the global standard CRS commonly used in GPS applications. At this point, it is worth noting that critical consideration in this workflow is that the clipping may require prior reprojection to match the CRS of the input EO raster data, which is a mandatory step for the clipping operations, it is significantly more efficient to perform this transformation on the SHP geometry rather than on the complete EO raster dataset. This approach not only optimizes processing efficiency by mitigating potential memory overflow issues that frequently arise when reprojecting large raster files.

Following reprojection, the ODC framework calculates several spectral indices commonly used in remote sensing applications (see **Table 5**). The automation of this integration provides an important advantage by delivering analysis-ready data, which can be immediately employed for coastal monitoring or other applications, without requiring high-demanding post-processing. However, it should be noted that these computational operations proportionally increase the final product size relative to the spatial extent of the clipping boundary. In cases involving large study areas, this may lead to substantial file sizes that warrant consideration during storage planning and data distribution.

The harmonization phase ends by combining all derived products with the original data, **generating the ODC product**. At this moment, the final product of the harmonization phase can be exported as NetCDF, which is an established standard for multidimensional scientific data storage and exchange. According to the application, the structure of a NetCDF file can be implemented using different architectural approaches. Precisely, for applications involving data distributions through sFTP networks with subsequent processing or visualization in GIS software (i.e., QGIS), the NetCDF structure needs to mimic a Virtual Raster (VRT) template

architecture. However, when GeoServer compatibility is required, an alternative layered structure must be employed, where each spectral image is stored as a separate dataset within the NetCDF file due to GeoServer's lack of VRT-based architecture. This architectural flexibility allows the ODC framework to adapt to various deployment scenarios while maintaining data integrity and accessibility.

Table 5. The ODC products

Band Name	Abbreviation in Product	Calculation	Sentinel-2 Band ID	Landsat-8/9 Band ID
Coastal Aerosol	coastal aerosol	RAW DATA	1	
Blue	blue	RAW DATA	2	
Green	green	RAW DATA	3	
Red	red	RAW DATA	4	
Vegetation Red Edge	vre	RAW DATA	5, 6, 7	X
Near-Infrared	nir		8	5
Narrow Near-Infrared	narrow nir	RAW DATA	8A	X
Water Vapour	water vapour	RAW DATA	9	X
Short-Wave Infrared Cirrus	swir-cirrus	RAW DATA	10	9
Short-Wave Infrared	swir	RAW DATA	11, 12	6, 7
Panchromatic	panchromatic	RAW DATA	X	8
Thermal Infrared Sensor	tirs	RAW DATA	X	10, 11
Normalized Difference Vegetation Index	ndvi	$\frac{nir - red}{nir + red}$	13	
Green Normalized Difference Vegetation Index	gndvi	$\frac{nir - green}{nir + green}$	14	
Red Edge Normalize	ndre	$\frac{narrow\ nir - vre}{narrow\ nir + vre}$	15, 16, 17	X

Difference Vegetation Index				
Enhanced Vegetation Index	evi	$\frac{2.5x(nir - red)}{nir + 6\ x\ red - 7.5\ x\ blue + 1}$	18	
Modified Soil Adjusted Vegetation Index 2	msavi2	$\frac{2\ x\ nir + 1 - \sqrt{(2\ x\ nir + 1)^2 - 8\ x\ (nir - red}}{2}$	19	
Modified Triangular Vegetation Index 2	mntvi2	$\frac{1.5\ x\ (1.2x(nir - green) - 2.5x(red - green)}{\sqrt{(2\ x\ nir + 1)^2 - (6\ x\ nir - 5\ x\ \sqrt{red}) - 0.5}}$	20	
Triangular Greenness Index	tgi	$\frac{120.0\ x\ (red - blue) - 190.0\ x\ (red - green)}{2}$	21	
Vegetation Condition Index	vci	$\frac{ndvi - \min(ndvi)}{\max(ndvi) - \min(ndvi)}$	22	
Normalized Difference Water Index	ndwi	$\frac{green - nir}{green + nir}$	23	
Modified Normalized Difference Water Index	mndwi	$\frac{green - swir}{green + swir}$	24, 25	
Water Ratio Index	wri	$\frac{green + red}{nir + swir}$	26, 27	
Land Surface Water Index	lswi	$\frac{nir - swir}{nir + swir}$	28, 29	
Normalized Difference Turbidity Index	ndti	$\frac{red - green}{red + green}$	30	
Automated Water Extraction Index	awei	$4\ x\ (green - swir2 - 0.25\ x\ nir + 2.75\ x\ swir1)$	31, 32	
Oil Spill Index	osi	$\frac{red + green}{blue}$	33	
Normalized Burn Ratio	nbr	$\frac{nir - swir}{nir + swir}$	34, 35	
Burned Area Index	bai	$\frac{1}{\left(0.05 - \frac{red}{\max(red)}\right)^2 + \left(0.02 - \frac{nir}{\max(nir)}\right)^2}$	36	

Normalized Difference Build-Up Index	ndbi	$\frac{swir - nir}{swir + nir}$	37, 38	
Bare Soil Index	bsi	$\frac{nir - 2\ x\ red + blue}{nir + 2\ x\ red + blue}$	39, 40	
Atmospherically Resistant Vegetation Index	arvi	$\frac{nir - 2\ x\ red + blue}{nir + 2\ x\ red + blue}$	41	
Visible Atmospherically Resistant Index	vari	$\frac{green - red}{green + red - blue}$	42	
Normalized Difference Snow Index	ndsi	$\frac{green - swir}{green + swir}$	43, 44	
Normalized Difference Chlorophyll Index	ndci	$\frac{vre - red}{vre + red}$	45, 46, 47	X
Floating Algae Index	fai	$narrow\ nir - (red + (swir - red)\ x\ 0.211640$	48, 49	X
Plastic Index	pi	$\frac{nir}{nir + red}$	50	
Land Surface Temperature [48]	lst	$L_\lambda = M_L\ x\ tirs + A_L$ $lst = \frac{K_2}{\ln\left(\frac{K_1}{L_\lambda} + 1\right)}$ M_L = RADIANCE_MULT_BAND_x from Landsat MTL file A_L = RADIANCE_ADD_BAND_x from Landsat MTL file K_1 = K1_CONSTANT_BAND_x from Landsat MTL file K_2 = K2_CONSTANT_BAND_x from Landsat MTL file	X	51, 52

2.2.2.3 Post Processing and Storage Management

The ODC framework produces analysis-ready products through the aforementioned semi-automated processing steps, described in the previous paragraphs. This design allows users to focus exclusively **on post-processing and data management tasks** tailored to their exact application requirements. For example, in a coastal monitoring application, post-processing primarily involves the generation of appropriate color palettes to provide effectiveness in the

visualization of spectral indices or other EO products. In addition, the framework's automated approach significantly reduces pre-processing overhead while maintaining flexibility for parameter customization during the harmonization phase.

Another functionality of the ODC framework is the incorporation of storage management within the harmonization phase, while maintaining user flexibility in data organization. The system automatically structures output products into directory hierarchies based on filename keywords, while the user retains full control over the physical storage location. Following product generation, distribution methods can be customized according to application needs. Options include sFTP transfer for complete dataset sharing or GeoServer deployment for selective band distribution. While the framework facilitates these common distribution pathways, it remains compatible with external storage solutions such as cloud platforms or public servers, as these implementation-specific choices are beyond the framework's core functionality.

2.2.2.4 Visualization of DC

The **Visualization of the ODC products** is the final step of the workflow. Nowadays, there are several technologies that enable the visualization of high-dimensional data in various forms.

To keep the analysis simple, this research compares traditional $3D$ $(band\ x\ latitude\ x\ longitude)$ or $4D$ $(time\ x\ band\ x\ latitude\ x\ longitude)$ data structures with a $5D$ data structure, whereas the 5th dimension is considered the elevation.

Thus, the final 5D data structure corresponds to the following dimensions $(time\ x\ DEM\ x\ band\ x\ latitude\ x\ longitude)$.

The visualization phase can be supported by a variety of software, such as GIS, 3D Editors, or Game Engines. Each software provides a unique environment with the necessary tools for visualizing, editing, or navigating over the 3D spatial environment by either selecting different dates (4th dimension, i.e., time) or different spectral perspectives (5th dimension, i.e., spectral band selection). For example, in QGIS software, several plugins can be used to transform a DEM into a 3D map, and the user can navigate to other dimensions by selecting different layers.

In a 3D Editor, such as Blender, the heightmap can be used as a displacement map or modifier to transform a plane mesh into a realistic ground representation. In this case, the dimensions corresponding to the time and spectral bands are imported as mesh materials to the mesh geometry. Similarly, in a Game Engine, the 3D mesh geometry can be imported along with the images or spectral bands, which will be used as model materials. However, game engines support advanced graphic structures, lighting simulations, and a programming environment, which helps the user develop realistic and interactive maps.

3 ODC Data Storage and Exchange Framework

Within the context of the OCEANIDS project, the ODC products are shared with all consortium members to support follow-up tasks in **WP3** and **WP4** as outlined in the GA.

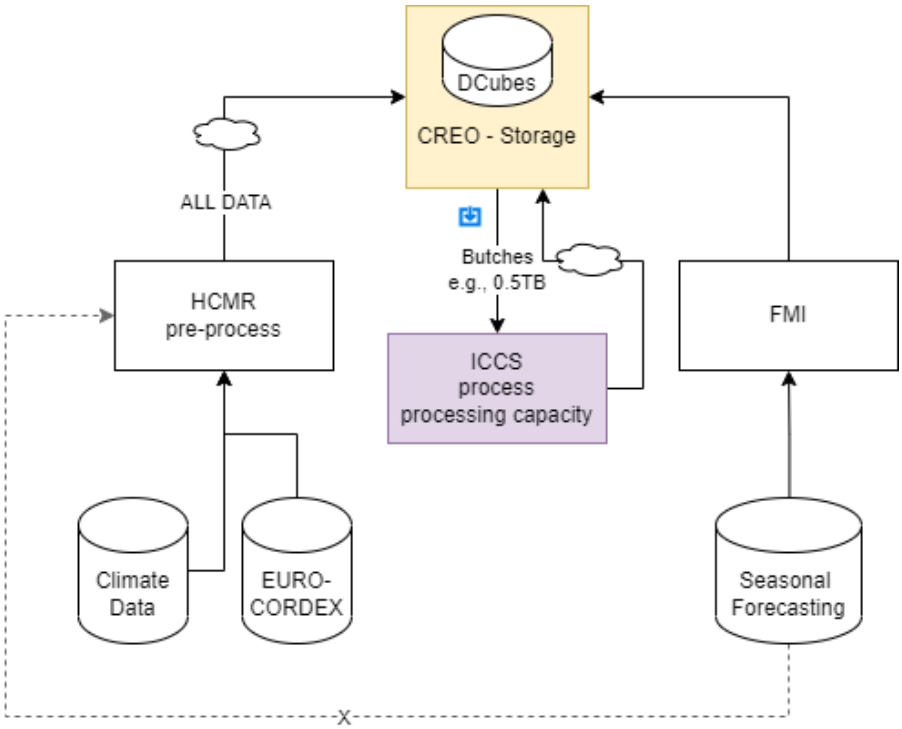

Figure 7. WP3 overall architecture.

In **Figure 7**, the overall architecture of the WP3 is depicted. The ODC products are generated inside the CREODIAS VM and stored inside the platform. To facilitate this, the architecture of the ODC framework was designed with an emphasis on data storage efficiency and interoperability, focusing mainly on: **(a) sFTP-based** data transfer among consortium members; and **(b) GeoServer** compatibility, enabling the dissemination of ODC products via standard WMS/WFS formats for both internal use and access by the end-users. The design of WP3 promotes **interconnectivity** not only within its internal tasks but also across other work packages. As shown in **Figure 8**, the flow of data and services among T3.1 (ODC), T3.5 (GeoServer), and WP4 (STAC catalogue for the platform) exemplifies this collaborative structure. The outputs from **T3.1** are made interoperable and accessible through the tools developed in **T3.5**, which in turn feed directly into the catalogue and visualization systems in **WP4**. This ensures a consistent and traceable pipeline from raw data pre-processing to user-facing applications. By enabling cross-WP data exchange and service integration, the architecture reinforces the project's modularity and scalability, while ensuring that each component contributes to the overall functionality of the OCEANIDS platform.

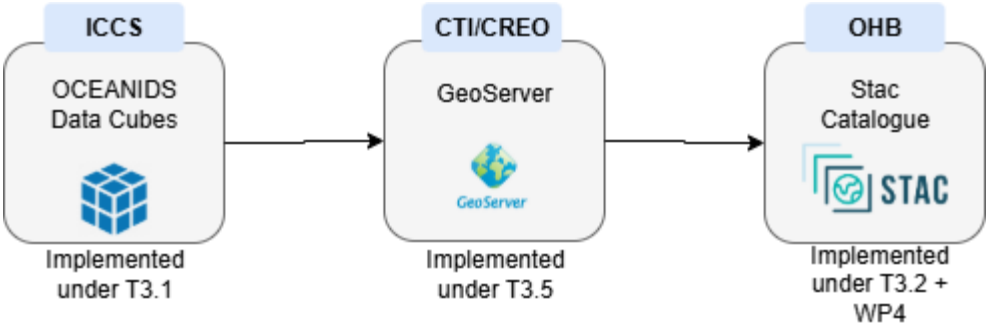

Figure 8. Direct connection between T3.1, T3.5 and WP4.

3.1 Data Storage Management

The ODC framework provides data storage efficiency by filtering only the necessary information from the raw datasets. This is achieved using geolocation parameters that define the area of interest by clipping the raw data over the specific regions. Especially for climate data, the framework uses only a central coordinate (i.e., lat, lon) to locate the center pixel of the CORDEX dataset. The surrounding information is then retrieved by specifying the size of the output grid (i.e., $2x2$, $3x3$, etc.).

For the case of EO data, the framework needs a shapefile geometry bounding the area of interest to identify the clipping geometry. While in most cases, the generated ODC product will have less size than the original data, it is worth noting that if the user needs large areas, then the final product will tremendously exceed the original size. This limitation exists because the harmonization process produces data under the same spatial resolution, thus it downscales specific spectral bands to a higher resolution. As a solution to this problem, the ODC framework provides the option for the users to select between three types of resolutions (i.e., HIGHEST, MEDIUM, and LOWEST).

Considering the current challenges of EO Big Data analysis, this approach provides efficiency, follows the open standards, and generates ready-to-use products for various applications. In most applications, the area of interest is small, thus the highest possible resolution (i.e., 10m for Sentinel-2 and 15m for Landsat-8/9 missions) can be used without storage issues. Thus, in terms of storage management, the current architecture of the ODC framework is trustworthy, efficient, and compatible with the open standards.

3.2 Data Exchange via sFTP transfer

Data exchange between consortium members is a critical process to ensure compliance with the GA by successfully implementing the project's tasks. To support this, the ODC products are designed to meet compliance requirements. As previously mentioned, the ODC products are optimized for storage efficiency, allowing them to be easily stored on a server and transferred via sFTP access among consortium members. **Figure 9** illustrates an example of data exchange using FileZilla and sFTP access provided by the OCEANIDS partner CREOTECH.

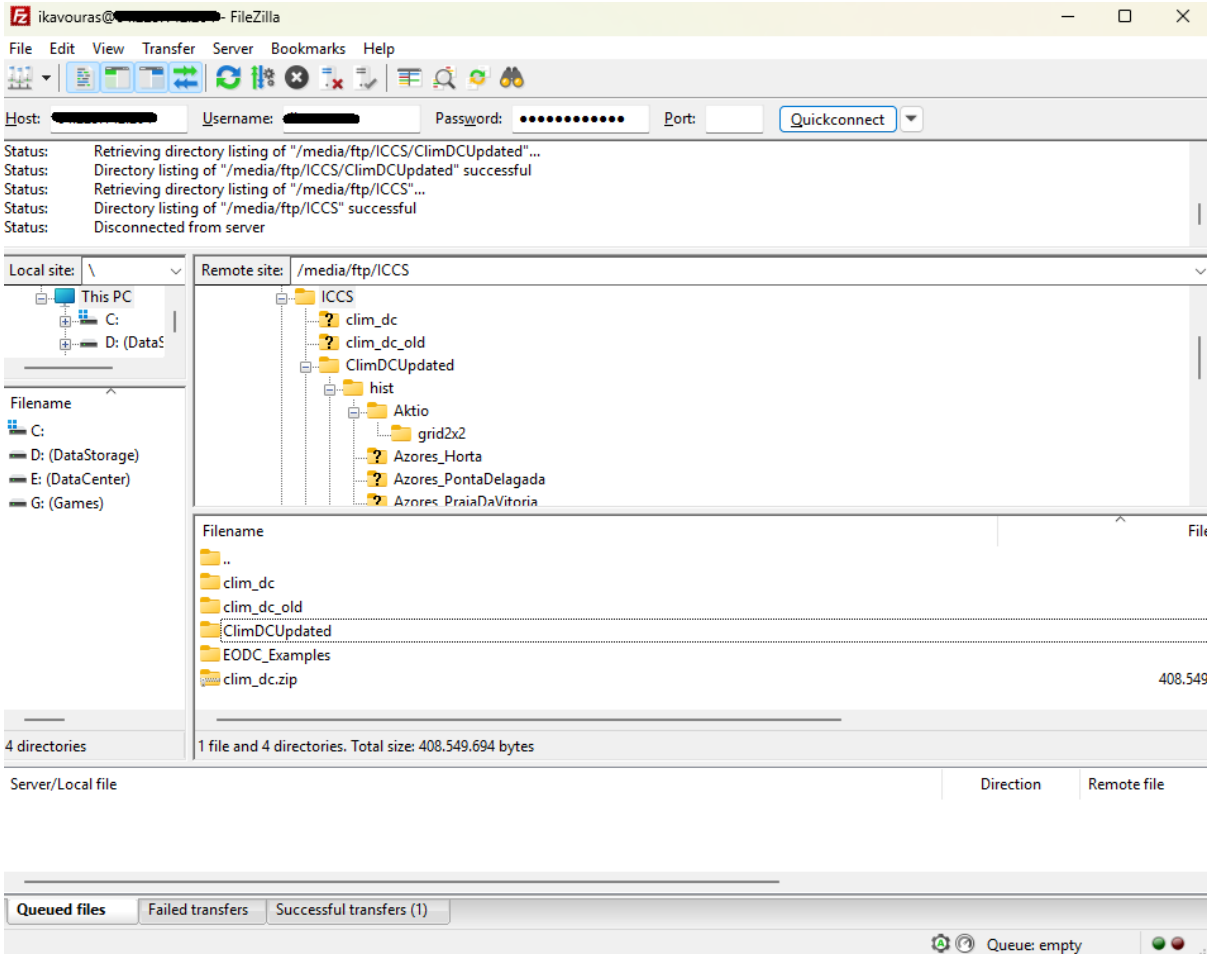

Figure 9. Data Exchange via sFTP transfer using FileZilla

3.3 Data Exchange via GeoServer

GeoServer compatibility is ensured by following the related template. Precisely, the Climate and Seasonal/Meteorological ODC products are distributed in NetCDF files following a 3D architecture $(time, latitude, longitude)$ that is compatible with the dedicated GeoServer created by CREO within WP3 in T3.5. The EO ODC products need to follow a 2D layer template $(latitude, longitude)$ as $band$ dimension is not recognized by GeoServer; thus, each spectral band lies as a different variable inside the NetCDF file.

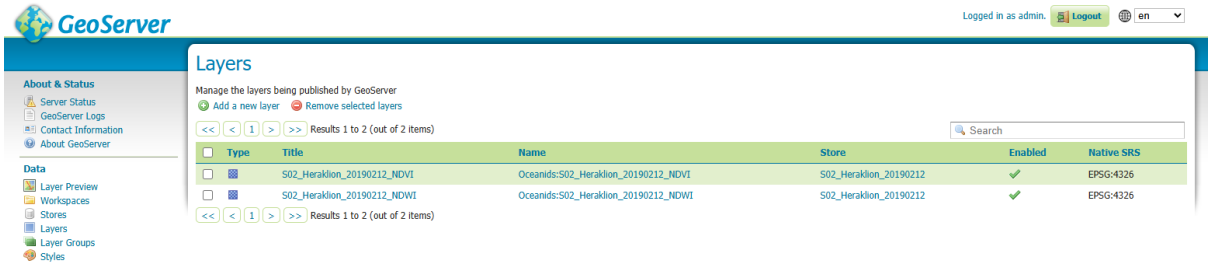

Figure 10. Example of a Sentinel-2 product inside the GeoServer. In this example the NDVI and NDWI layers have been created for distribution.

Figure 10 illustrates an example of ODC products inside the GeoServer. The creation and distribution of each layer can be handled from the GeoServer's administrative page (**Figure 11**) by selecting the "Publish" option for non-published layers. Each published layer can be previewed inside the interface of the GeoServer as shown in **Figure 12**.

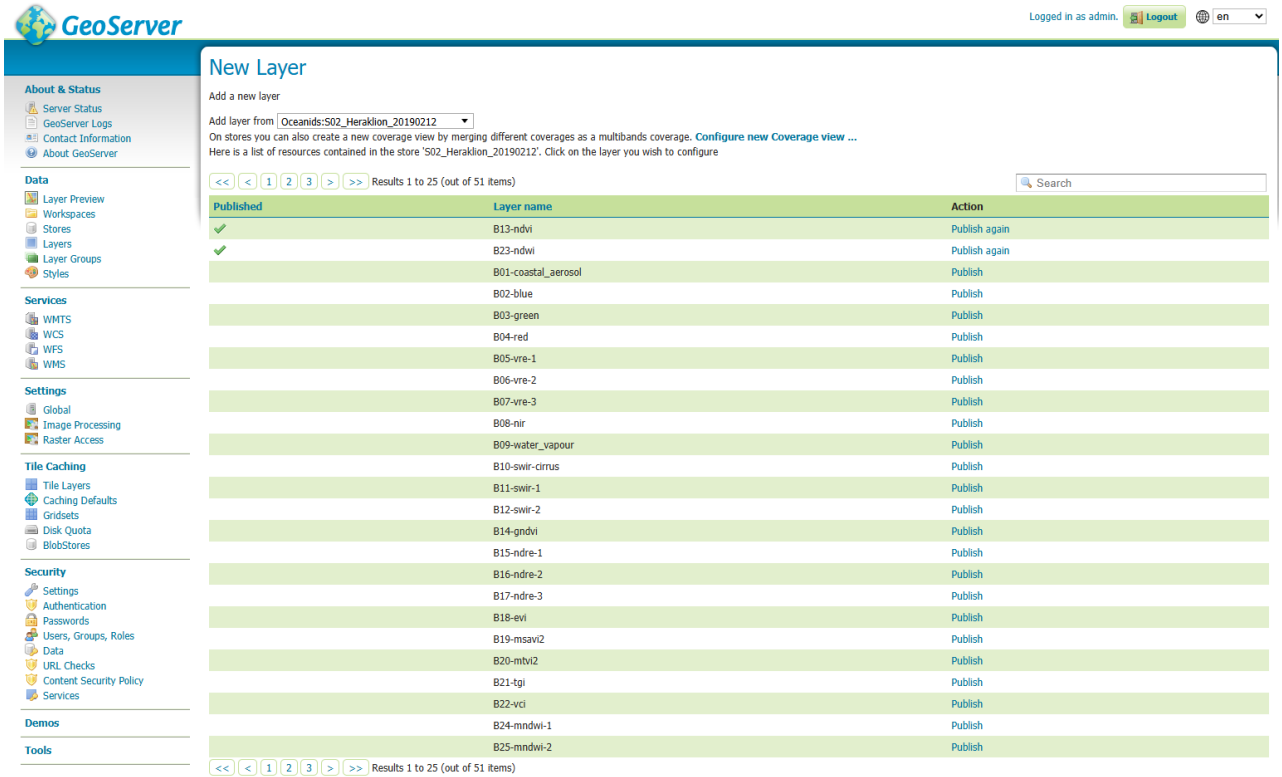

Figure 11. New Layer creation panel inside the GeoServer. This is an administrative page, which allows the creation and distribution of layers.

Figure 12. Visualization of NDVI layer inside GeoServer

Finally, the products can be accessed following the WMS/WFS settings inside any GIS software to visualize the products. **Figure 13** provides a demonstration of the NDVI layer overlaid over the Google Maps basemap inside QGIS. The layer has been retrieved via WMS access from the GeoServer.

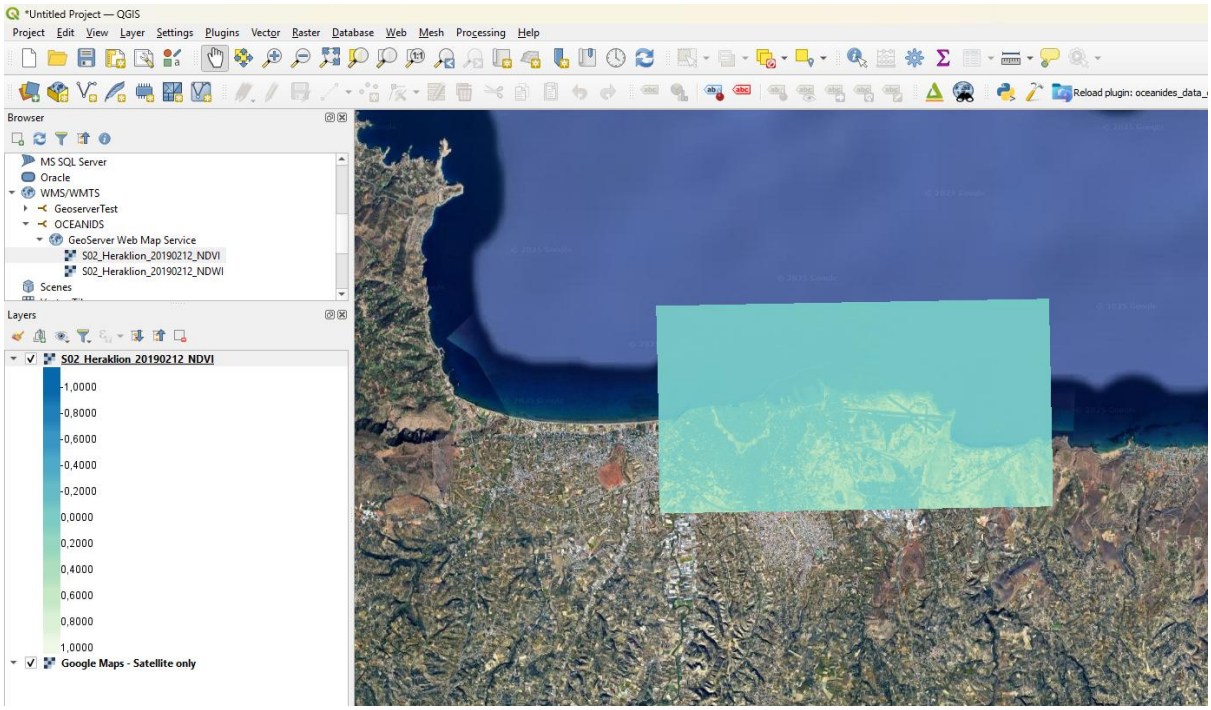

Figure 13. Visualization of GeoServer's NDVI layer inside QGIS and overlayed over Google Maps basemap.

4 Demonstration of ODC Applications

Following the previous sections, the ODC products can be used for several applications related to maritime, coastal, and climate change monitoring. Examples of these applications include: **(a)** Disaster monitoring in coastal areas; **(b)** Monitoring port degradation parameters; and **(c)** Climate and Seasonal/Meteorological data downscaling. The following paragraphs provide examples of such applications.

4.1 Disaster monitoring in coastal areas - Monitoring the oil-spill disaster in Saronikos Gulf in September 2017

On the 10th of September 2017, the tanker "Agia Zoni II" sank southwest of Atalanti Island, near Salamina Island, causing an oil spill of great magnitude in the surrounding marine and coastal areas[49]. This disaster indicates the necessity of developing tools and products that can help both local authorities and related end-users to effectively identify, monitor, and manage such a crisis. ODC products contain ready-to-use products for water regions monitoring, like NDWI, WRI, and OSI, which can effectively be used for marine and coastal monitoring.

This demonstration provides an analysis based on ODC products for monitoring the time period before the oil spill (2016 to 9th of September 2017), some days/weeks after the oil spill (10th of September to October 2017), and later years (2023-2024), using EO data (Sentinel-2 and Landsat-8/9 missions). The ODC original data consists of 16 satellite imagery products (5 from Landsat-8/9 and 11 from Sentinel-2), while for visualizing the oil-spill NDWI, WRI, and OSI indices used for monitoring the quality of the Saronic Gulf during the aforementioned periods.

Figure 14 illustrates the results based on the ODC products. This visualization was achieved inside QGIS software and considers the Visible RGB color composition, NDWI, WRI, and OSI indices using color maps, following the calculations of **Table 5**. The results indicate that NDWI values usually range between $[0.0, 0.2)$ visualizing the humidity levels over the Saronic Gulf. The 13th of September 2017 is an exception to the aforementioned observation, indicating the abnormality of the oil spill in the middle of the Saronic Gulf.

Similarly, the WRI index allows the observation of a periodic phenomenon (black regions) along the coastline of Salamina island. During the oil spill event, the region inside the green box shows dark spots in the sea level, which indicate oil-spill pollution. However, it is worth noting that only Sentinel-2 (10m/px resolution) captures these phenomena, while Landsat-8/9 (15m/px to 30m/px) cannot be used for this application.

OSI produces interesting results between Landsat-8/9 and Senintel-2 original products. By using the same values for the same range of data, it seems that ODC products from the Landsat-8/9 mission distinguish the area into water body, vegetation, and building/infrastructure. However, Sentinel-2 provides better resolution, allowing the monitoring of vegetation and building/infrastructure areas (orange/red colors) and differences in water bodies (yellow to blue colors) (**Figure 14**).

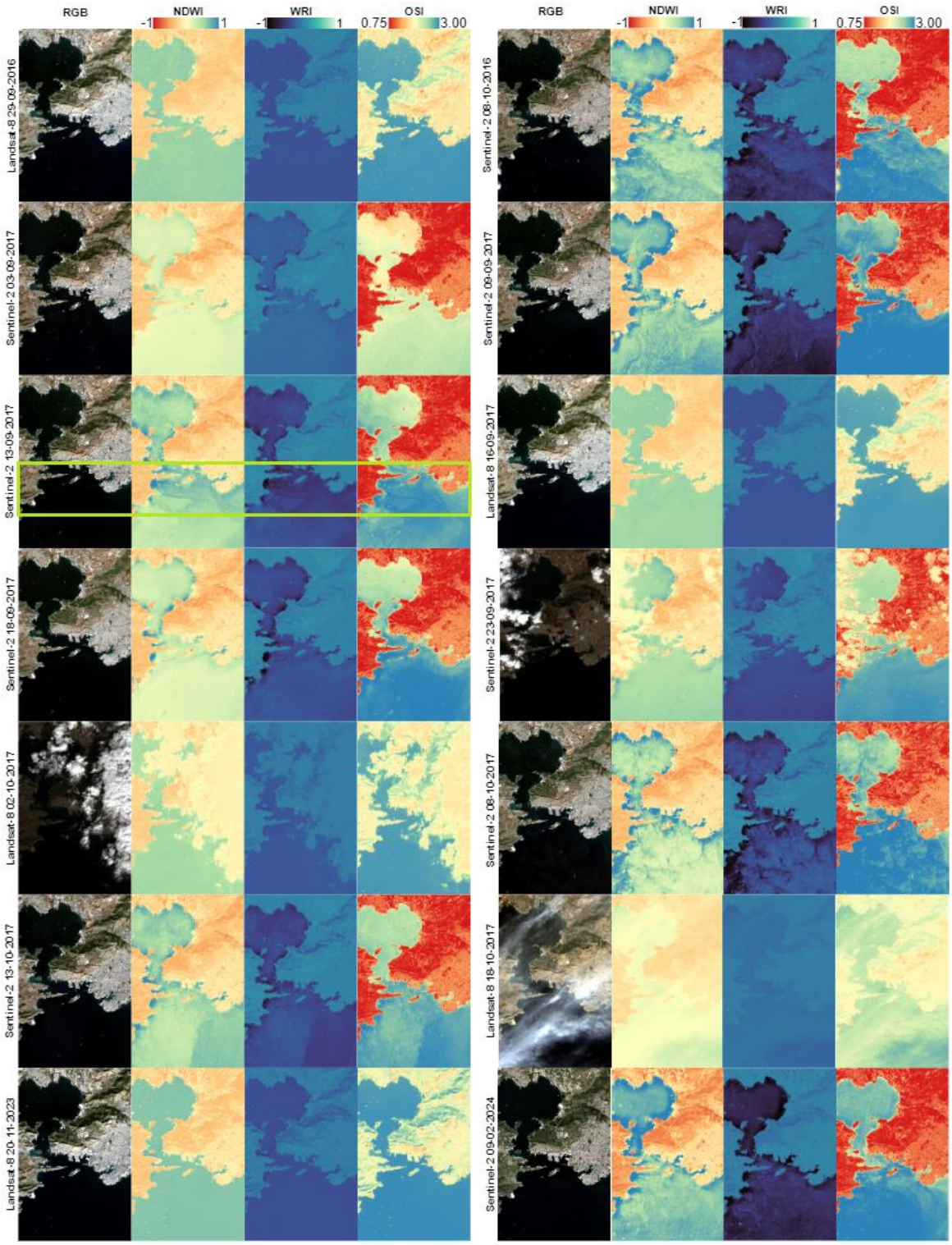

Figure 14. Time series monitoring the water quality of Saronikos gulf before and after the oil-spill using the RGB, NDWI, WRI and OSI products of the ODC framework. The green box indicates the critical area of identified oil-spill.

By combining the information of the three products, it is feasible to identify critical areas inside the green boundary. In addition, the time-series analysis of this example indicates other periodic phenomena in the Saronic Gulf, like the recursive pattern of dark pixels in NDWI and

WRI in the Salamina coastline, which is not correlated with the oil-spill disaster as it appeared before the event and in recent years.

4.2 Monitoring port degradation parameters – Monthly monitoring of Crete and Port of Heraklion area from January 2016 to December 2024

An important application related to the ODC products is the monitoring of coastal degradation. To demonstrate the effectiveness of this application, Crete Island (one of the pilot regions of the OCEANIDS project) was selected as the area of interest. The port of Heraklion is a critical hub for Crete's blue economy; thus, the Heraklion Port Authority manages the following principal maritime activities: (a) ferry operations; (b) cargo handling; (c) cruise tourism; (d) fishing harbor services; and (e) shipyard maintenance. This multifaceted operations underscore the port's strategic economic importance while simultaneously increasing its vulnerability to coastal environmental changes that could impact maritime infrastructure and operations. The following sections describe in detail the experimental setup and results following the pipeline of the ODC framework.

The demonstration investigates the core environmental parameters that can be easily identified using remote sensing products and act as indicators of coastal degradation, especially in the **Port of Heraklion**. *According to the European Commission, there are several variables that could be useful for coastal degradation monitoring*. A brief description of these variables is provided below:

1. **EXTREME WIND SPEEDS AND WAVES**: These data can be collected from climate or meteorological models from online sources or in-situ data collection using local stations.
2. **SEA LEVEL**: These data can be expressed as seasonal or annual variability, considering local tectonics, subsidence, or uplifting of the coast. Tidal trends are also included in these data categories.
3. **CLIMATE/METEOROLOGICAL VARIABLES**: The data can include climate/meteorological phenomena, variables, and parameters such as temperature, humidity, precipitation, barometric forcing, etc. These datasets are mostly provided by models. However, some of these parameters, such as temperature, can be collected, calculated, or provided in EO data (i.e., TIRS bands in Landsat-8/9).
4. **COASTAL GEOLOGY**: Coastal geology can be monitored using the SWIR bands of EO data (i.e., Landsat-8/9 and Sentinel-2) or geological maps.
5. VERY HIGH-RESOLUTION **BATHYMETRY DATA**.
6. **VEGETATION IN THE COASTAL ZONE**: By calculating the NDVI or NDWI EO products, it is possible to monitor coastal vegetation both underwater and onshore. Vegetation can stabilize the seabed and coastal dunes.
7. MONITORING OF **DELTAS, LAGOONS, VEGETATION, MARSHES**: These parameters can be monitored using EO data (i.e., Landsat-8/9 and Sentinel-2).
8. **RIVER DISCHARGES AND SEASONAL RIVER-BORNE SEDIMENT LOAD**: Similarly, these parameters can be monitored using EO data such as Landsat-8/9 and Sentinel-2.

Considering these variables, the appropriate data collection strategy is designed. Most of these variables can be visualized using EO data, such as Sentinel-2 and Landsat-8/9. Sentinel-2's superior 10-meter spatial resolution makes it ideal for coastal monitoring, though it lacks thermal bands for temperature analysis. For this demonstration, monthly Sentinel-2 data from January 2016 to December 2024 and monthly Landsat-8/9 data from January 2024 to December 2024 were downloaded for thermal analysis and cross-sensor comparison. A significant challenge associated with both satellite systems is cloud interference, which can obscure critical ground observations. To address this, a cloud cover threshold of 60% was applied during data selection to maximize the availability of usable scenes while minimizing the impact of cloud obstruction.

Figure 15. Polygon geometries of selected areas of interest. (a) Red boundary is used for clipping the whole Crete Island; (b) Yellow boundary is used for clipping the coastal area around the Port of Heraklion.

Additional data includes the shapefile geometries that are used for clipping the EO data and representing the areas of interest. **Figure 15** illustrates these boundaries: **(a)** The **red boundary** is used for clipping the images around Crete Island; and **(b)** The yellow boundary is used for clipping the images around the Port of Heraklion. At this point, it is important to note that if the defined boundary extends beyond the extent of the EO images, the clipping area is automatically reduced to fit within the image boundaries. In this case, the selected Sentinel-2 images cover the northern coastal area of Crete Island, and therefore, the analysis focuses specifically on that region. Additionally, the SRTM 1 Arc-Second Global DEM for Crete Island was downloaded from the USGS Earth Explorer. This dataset is used to generate the third spatial dimension (elevation) in the analysis.

The harmonization phase uses the tools of the ODC framework[47] for generating **two types of data cubes**: **(a)** Layered data cubes compatible with Geoserver; and **(b)** VRT-based data cubes for GIS software processing. Please note that these types of data cubes can be used in combination with each other for high-dimensional processing. For example, **Figure 16** illustrates a 5D visualization of the NDVI difference in Port of Heraklion from February 2019 to February 2022, indicating the potential of the proposed methodology.

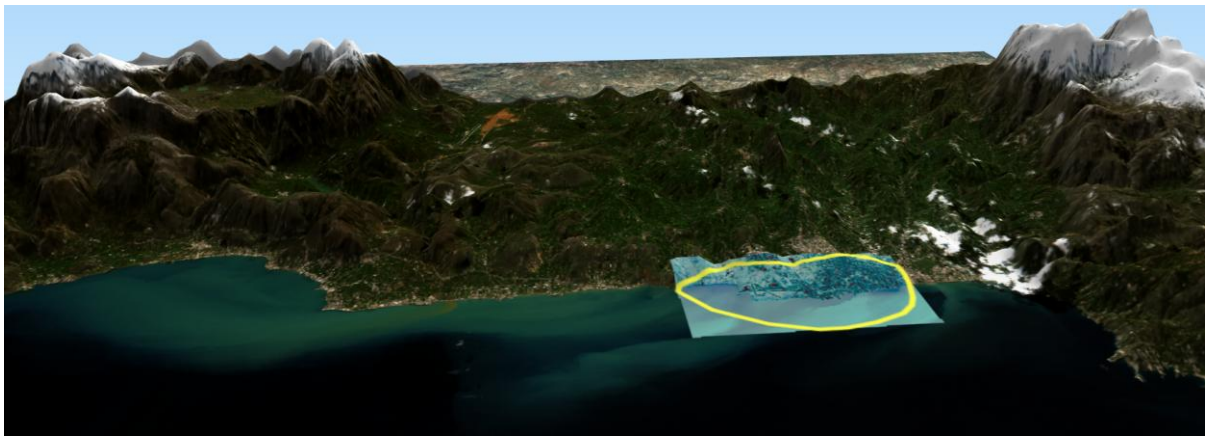

Figure 16. 5D (3 spatial, 1 temporal, and 1 spectral) visualization of the NDVI difference in Port of Heraklion from February 2019 to February 2020.

An alternative approach for achieving similar results involves generating a mesh model within a 3D editor and applying the ODC as a material texture. This method offers greater flexibility, as 3D editors provide tools and visualization capabilities not typically available in GIS software. An extension of this approach is the use of a game engine environment for visualization and analysis. Game engines support advanced features such as programming, simulation, and high-fidelity graphics (e.g., particle systems), which can be leveraged to further enhance the dimensionality and interactivity of the visualizations.

To evaluate the efficiency of the ODC framework for periodic coastal monitoring and compare it with the state-of-the-art approaches, five evaluation metrics were defined:

1. **STORAGE RATIO (SR)**: The SR is calculated by dividing the ODC product's size by the raw product's size, when both of these products contain the same spectral information (i.e., bands). This metric provides insights related to storage management.
2. **TIME PERFORMANCE RATIO (TPR)**: This metric is calculated by comparing the time needed to calculate the products by standard methods (e.g., manual approach using GIS software or automation when it exists in GIS software).
3. **PPRODUCTS QUALITY/RESOLUTION (PQR=low, medium, high)**: This metric compares the products created from the ODC framework with those created by standard methods.
4. **VISUALIZATION RESULTS (VisRes=low, medium, high)**: This metric evaluates the different dimensional products in terms of visualization. The evaluation criteria are the ease of detection of the different entities (i.e., vegetation, urban, coastal areas, etc.) in the images, without further processing.
5. **IDENTIFYING CRITICAL CONDITIONS (ICC=easy, medium, hard):** This metric is an extension of VisRes. In this case, different dates are visualized together for identifying trends related to seasonal or yearly changes and identifying outliers or critical conditions of potential degradation.

4.2.1 Results

As described in the previous section, the main objective of this case study is to identify degradation in the northern coastal area of Crete Island, with emphasis mostly on the surrounding area of the Port of Heraklion. By using the collected dataset, several EO products[50] were calculated following the ODC framework. According to the literature, the following products are the most suitable to monitor coastal degradation: **(a)** Visible Spectrum (RGB)[51]; **(b)** Visible Near Infrared (VNIR)[51]; **(c)** Visible Short-wave Infrared (VNIR-SWIR)[52]; **(d)** Thermal Infrared Products (i.e., Land Surface Temperature – LST)[52]; **(e)** Normalized Difference Vegetation Index (NDVI)[53], [54]; **(f)** Normalized Difference Water Index (NDWI)[53]; **(g)** Normalized Difference Build-up index (NDBI)[53], [54]; Oil Spill Index (OSI)[55]; and **(h)** Normalized Difference Red Edge Index (NDRE) [53]. **Figure 17** presents a brief visual example of the final products as stored within the system.

For the full dataset, a total of 120 products were calculated and visualized—12 from the Landsat-8/9 dataset and 108 from the Sentinel-2 dataset—for each product type (e.g., RGB, VNIR, NDVI, NDWI, etc.) and each clipping boundary. On average, processing a single raw product (either Sentinel-2 or Landsat-8/9) outside the ODC framework required approximately 90 minutes. In contrast, the same processing within the ODC framework took less than 10 minutes, demonstrating a substantial improvement in efficiency. Thus, the TPR metric is calculated as follows: $TPR = \frac{10}{90} = 0.11 = 11\%$ of the average time needed using traditional approaches (i.e., 89% less time).

Similarly, the following tables (**Table 6** and **Table 7**) present the results of the SR metric for the clipping with the Port of Heraklion and Crete geometries, respectively. It is worth noting that small geometries (i.e., coastal monitoring in a small radius around the port) reduce the storage size of the final products. However, in the opposite scenario—where large geometries are required (e.g., monitoring the entire northern coastal region of Crete)—the storage size of the final products increases significantly. To address this, it is recommended to properly format the data and organize the storage structure to prevent memory overflow and ensure efficient data management.

Figure 17. Samples of 4D (***time x bands x lat x lon***) analysis using ODC products for the Port of Heraklion. (a) Visible Spectrum; (b) Visible Near Infrared; (c) Visible Short-ware Infrared; (d) Normalized Difference Vegetation Index; (e) Normalized Difference Water Index; (f) Normalized Difference Build-up Index.

Continuing the analysis, **Figure 18** illustrates an example of periodic monitoring in the coastal area of the Port of Heraklion using a yearly temporal window created around February. By comparing the images across years, a significant accumulation of river debris is visible on February 26th, 2022, potentially indicating coastal degradation. This 4D analysis (*time x bands x lat x lon*), evaluated using the VisRes criteria, yielded high-quality visual outputs that facilitate the identification of critical conditions. Specifically, the ICC (Image Complexity and Clarity) metric was assessed as 'easy,' indicating a high level of interpretability.

Table 6. Storage Ratio Metric for Clipping with Port of Heraklion geometry ODC products.

Satellite Mission	Data Date Range	Data Raw Size [GB]	Size of product containing only raw bands [%]	SR of product containing only raw bands [%]	Size of product containing all bands (raw and calculated) [GB]	SR of product containing all bands (raw and calculated) [%]
Sentinel-2	Jan 1st, 2016, to Dec 31st, 2024	70.0	3.0	4.3% (decreased by 96.7%)	11.0	15.7% (decreased by 84.3%)
Landsat-8/9	Jan 1st, 2024, to Dec 31st 2024	11.0	0.14	1.3% (decreased by 98.7%)	0.50	4.5% (decreased by 95.5%)

Table 7. Storage Ratio Metric for Clipping with Crete geometry ODC products.

Satellite Mission	Data Date Range	Data Raw Size [GB]	Size of product containing only raw bands [%]	SR of product containing only raw bands [%]	Size of product containing all bands (raw and calculated) [GB]	SR of product containing all bands (raw and calculated) [%]
Sentinel-2	Jan 1st, 2016, to Dec 31st, 2024	70.0	3.0	4.3% (decreased by 96.7%)	11.0	15.7% (decreased by 84.3%)
Landsat-8/9	Jan 1st, 2024, to Dec 31st 2024	11.0	0.14	1.3% (decreased by 98.7%)	0.50	4.5% (decreased by 95.5%)

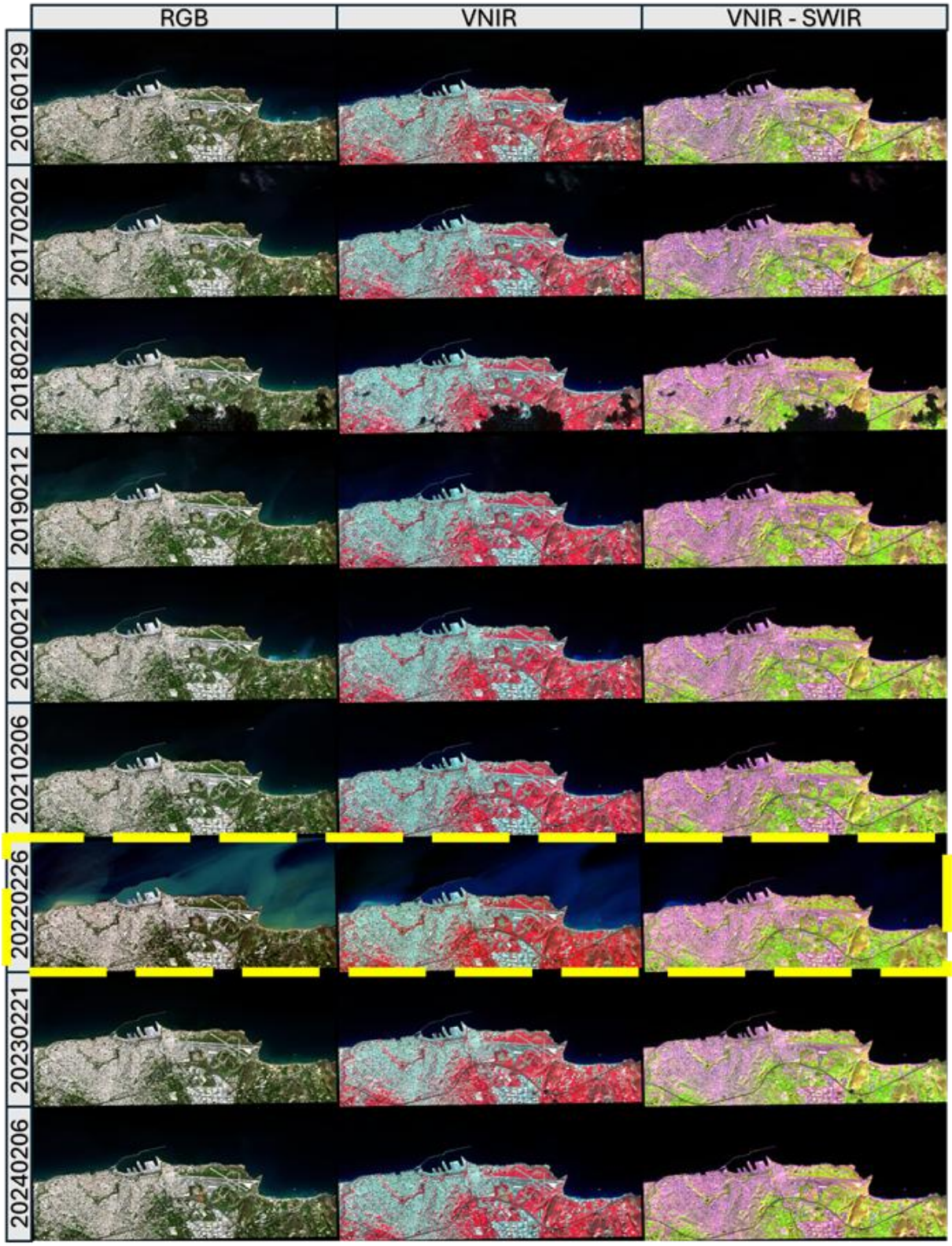

Figure 18. Example of periodic monitoring in coastal area of Port of Heraklion, using a yearly temporal window near February each year. The yellow boundary indicates critical condition and possible degradation in the coastal area.

Further analysis for estimating the magnitude of an extreme event uses EO indices products that are also provided in the ODC framework. **Figure 19** compares the NDVI, NDWI, NDBI, and OSI of February 26th, 2022 (critical conditions with a lot of river debris in the coastal area) with February 21st, 2023 (normal conditions – suitable for control image). The NDVI in both images is similar, with little difference in the agricultural area. In the NDWI products, the image of February 26th, 2022, indicates the critical areas with higher values (dark blue). Similarly, on February 21st, 2023, it appears that there is a small critical situation near the bay next to the airport. NDBI indicates some debris in the image of February 26th, 2022. This index is used for highlighting the manufactured built-up areas (higher values) and mitigating the effects of terrain illumination (lower values). The debris is visualized with a blue-ish color, indicating ground (probably dirt, gravel, rocks) material in the coastal area. Finally, the OSI index provides additional information about the water condition. In this index, the critical situation appears in the range 1.60-1.75 (dark purple) values, which appear in the image of February 26th, 2022, near the coastline. Clear or slightly dirty water appears between the ranges of 1.30-1.60 (1.30-1.45 clear, 1.45-1.60 slightly dirty).

The analysis so far expands the 3D ODC products to 4th dimension, which is the temporal ($time$) dimension. However, 5D mapping (i.e., $time\ x\ DEX\ x\ band\ x\ lat\ x\ lon$), simulations of phenomena and serious games for policy making[56] and decision support systems[57] are an emerging trend. For this reason, it is necessary to investigate the feasibility of using ODC in combination with 3D models, the ease of generating these models, and their final quality and resolution, which in this research is evaluated using the defined PQR metric.

Figure 20 provides an example of 5D visualization using QGIS. It is important to note that in the upper left corner, the user can select any given point of interest and view its 3D spatial information. Moreover, in this representation, the user can freely choose different temporal products for visualization in the Crete region and different ones for the Port of Heraklion. For example, in the case study, the Crete region was illustrated using the product of February 26th, 2022 (critical conditions), while the Port of Heraklion overlay changed between February 26th, 2022, and February 21st, 2023. Naturally, the number of possible variations is virtually unlimited, allowing the user the flexibility to select combinations that best suit the specific application.

Finally, using Landsat-8/9 products, it is possible to calculate the LST for identifying extreme temperatures that can affect the port infrastructure and cause material degradation. **Figure 21** illustrates the monthly LST of 2024 calculated by the ODC framework. Please note that in the Port of Heraklion, during the summer months, the temperature is between 30-35 degrees Celsius, which is high. In addition, during October and November, lower temperatures are observed, with some areas indicating extremely low temperatures. Thus, the combination of LST products with others can provide a complete analysis for ocean degradation monitoring.

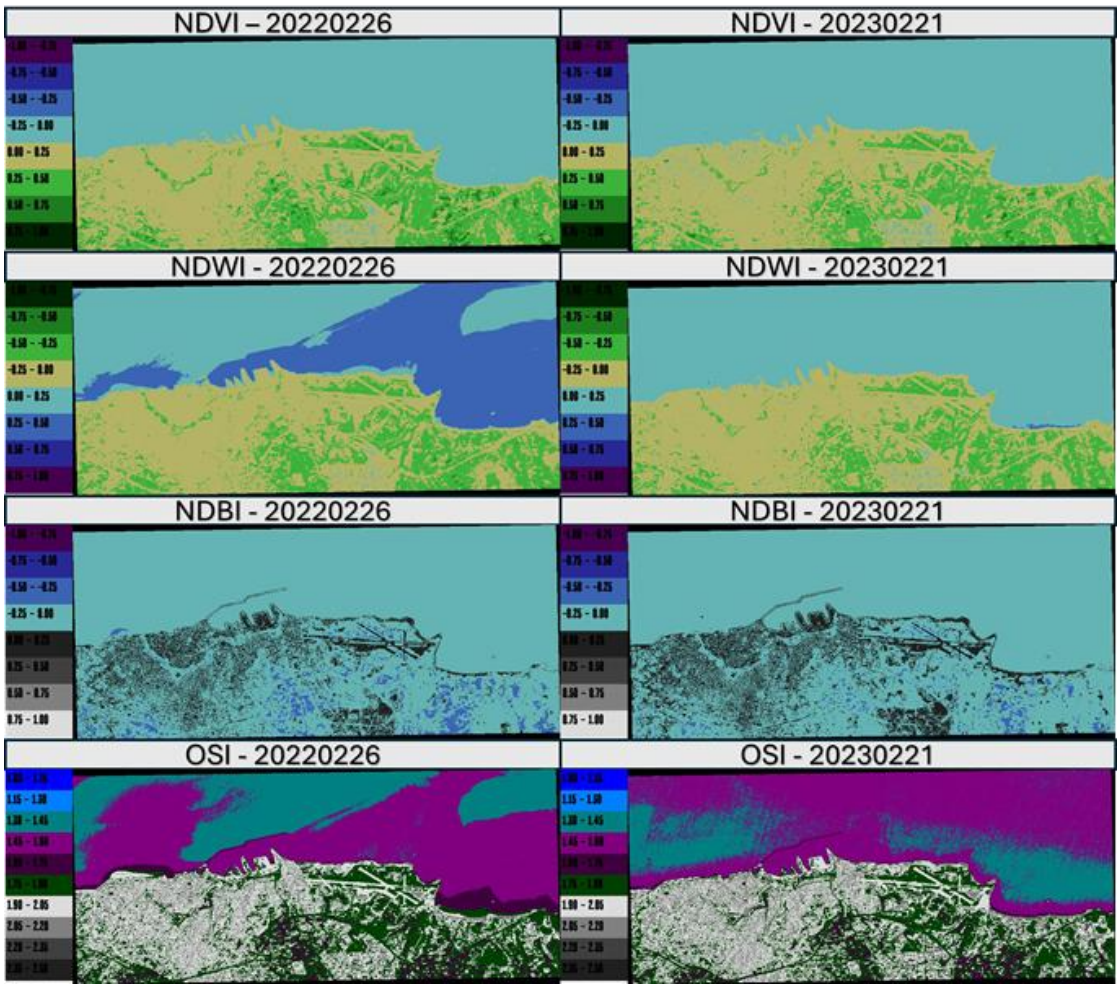

Figure 19. Comparison between the products of February 26th, 2022 (critical conditions) and February 21st, 2023 (normal conditions).

In terms of the PQR index, the quality of the products is high. In this case study, visualization of the 5D data cubes was performed using QGIS; however, as previously noted, other software tools are also compatible. To summarize, the proposed methodology has proven effective, and the ODC framework is capable of generating large volumes of data in a short time. These data can either be post-processed or used directly to produce multidimensional visualizations that highlight critical conditions potentially leading to coastal degradation.

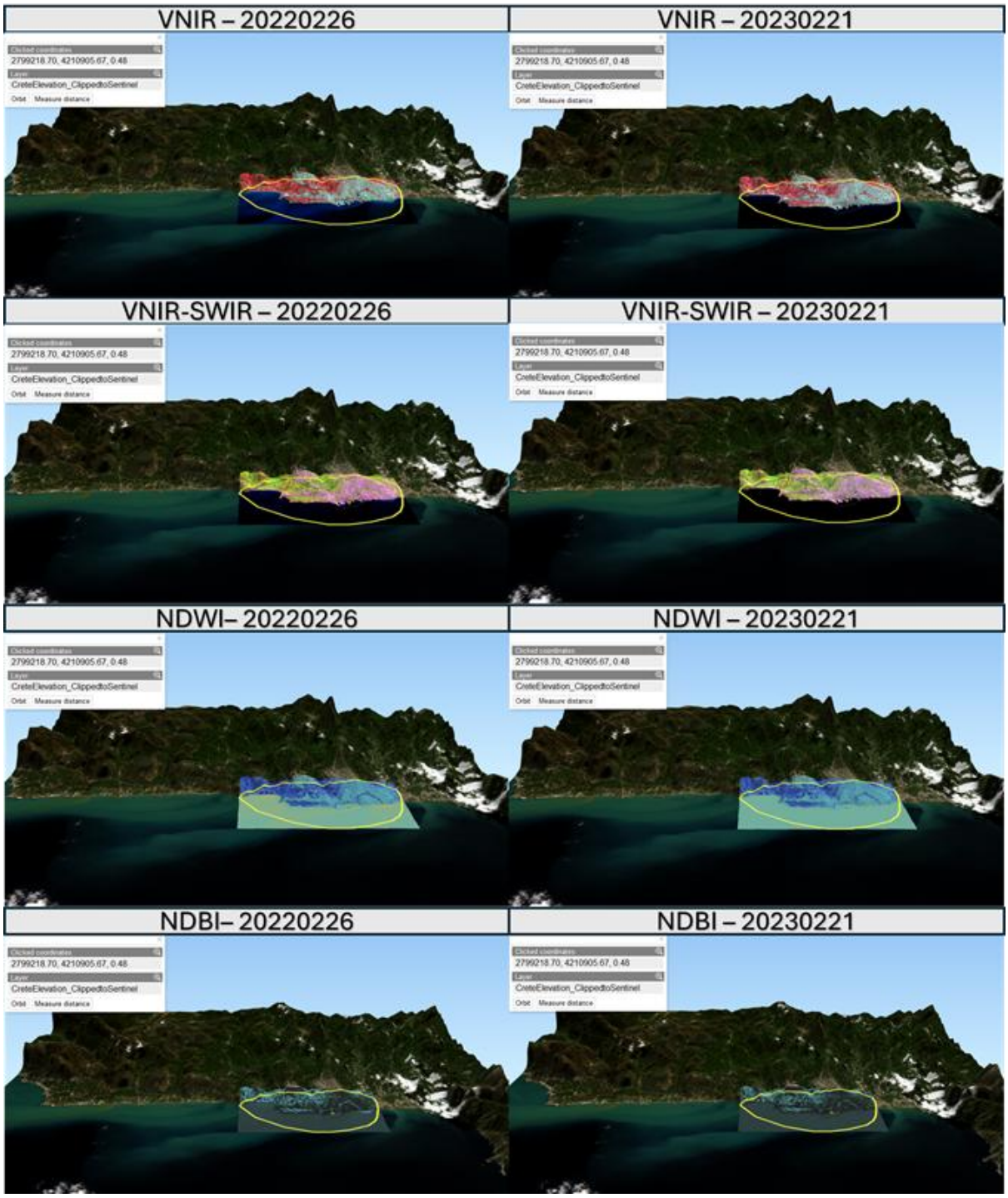

Figure 20. 5D visualization of ODC products inside QGIS.

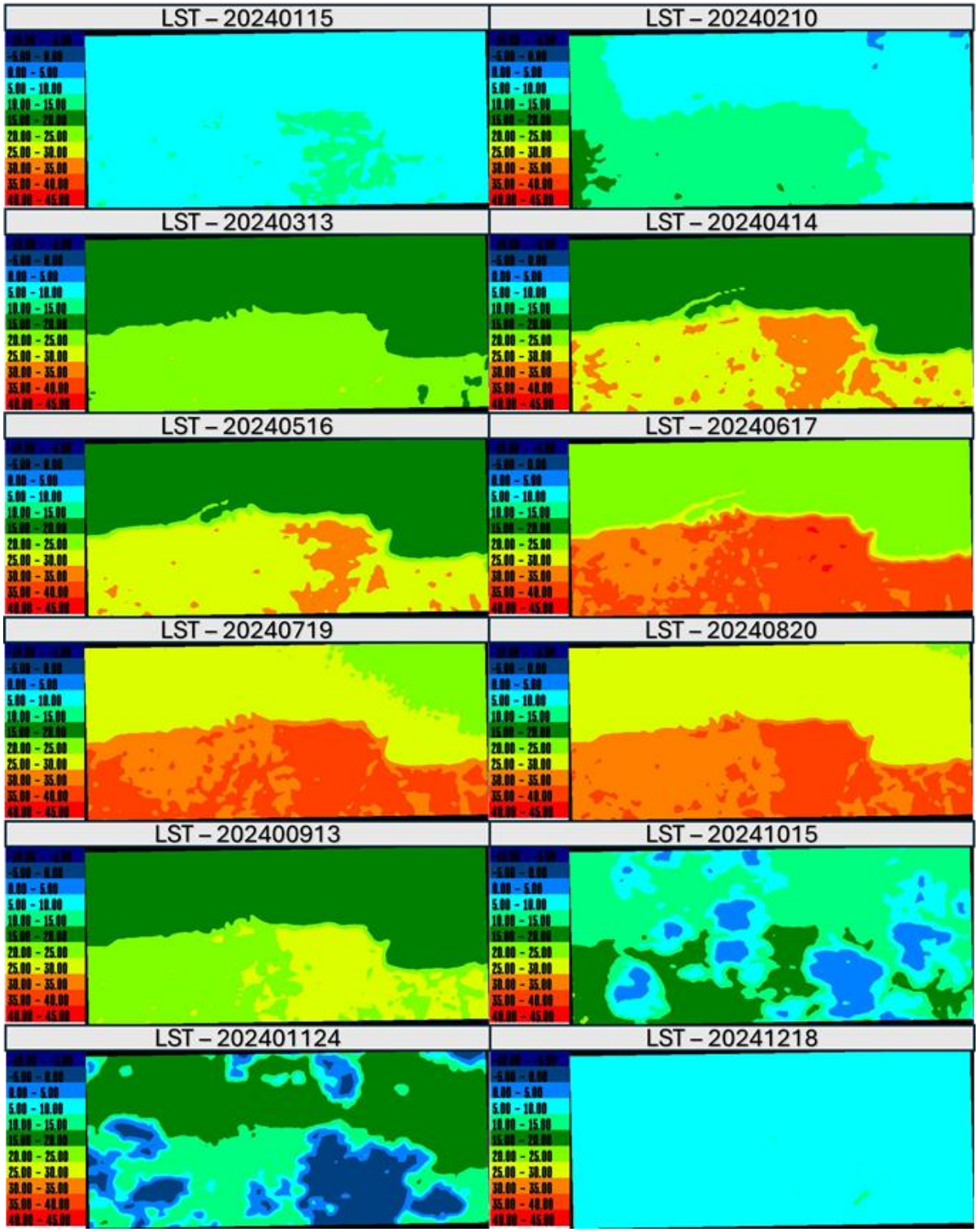

Figure 21. Land Surface Temperature 4D monitoring using Landsat-8/9 products.

4.2.2 Discussion

This study demonstrates the significant potential of the ODC framework for monitoring coastal surface degradation. In particular, the study emphasized port environments, where infrastructures are highly exposed to environmental (i.e., temperature, humidity, salinity, etc.) and anthropogenic (i.e., cargo management, cruiser/tourism/traveling activities, etc.) stressors. Through the integration of the ODC framework, the importance of data harmonization and multidimensional structuring and visualization of EO products can facilitate scalable and time-efficient analysis of long-term trends related to coastal resilience.

The experimental results of the case study in Crete and the Port of Heraklion underscore the added value of spatiotemporal analytics for the early detection of coastal degradation indicators. Both band combinations, like Visible RGB, VNIR, and VNIR-SWIR, along with indices calculations like NDVI, NDWI, NDBI, and OSI, provided reliable proxies in the identification of seasonal changes, erosion patterns, vegetation changes, and sedimentation anomalies, highlighting critical conditions. Notably, the 4D and 5D visualization capabilities of ODC allowed for intuitive interpretation of complex patterns across spatiotemporal and spectral dimensions that are critical for EWS and DSS in coastal management.

In addition, the evaluation metrics, and specifically the PQR, VisRes, and ICC criteria, demonstrated that ODC products not only meet the standards required for operational use but, in many cases, exceed them. The detection of extreme coastal events (e.g., river debris accumulation in February 2022) was immediate and visually discernible without additional processing, validating the effectiveness of the framework's automated processing and visualization pipeline. Furthermore, in terms of time (TPR), the ODC framework can accelerate processing analysis up to 89% by semi-automating the whole calculation/visualization processes (the user only needs to create the color maps and select which parameters they want to visualize). In terms of storage management, the ODC framework can handle efficiently the creation of data for small regions; however, for larger areas (i.e., the northern region of Crete), the product's size is hugely expanded. This limitation can cause serious storage issues (i.e., memory overflow); thus, it is not recommended to use this process analysis for large areas.

Finally, this work aligns with broader literature in remote sensing and environmental analytics, emphasizing the transition from static observation to dynamic and predictive monitoring. The ODC framework contributes to this transition by offering a generalized, adaptable, and on-the-fly system, which can be integrated with several kinds of data. The ODC framework was developed mainly for ocean and coastal applications, especially near port areas, but in reality, it can be used for other applications as well (i.e., vegetation monitoring, deforestation monitoring, urbanism monitoring, etc.). In addition, it can work well with artificial learning and machine learning applications, as the ODC products can be used as input/output with little to no post-processing.

Thus, future work will focus on enhancing the ODC framework through integration with predictive models and real-time data streams, while expanding its application to other sensitive coastal zones. Higher visualization dimensionality will also be investigated, possibly through simulations.

5 Conclusions

This deliverable presents a validated and operationally mature implementation of the ODC framework, designed to address the critical challenges of data heterogeneity, volume, and spatiotemporal complexity in environmental and climate monitoring. By harmonizing the diverse EO (i.e., Sentinel-2, Landsat-8/9, etc.) and non-EO (i.e., CORDEX climate projections) datasets, the ODC framework facilitates scalable, automated, and reproducible generation of multidimensional, analysis-ready products.

The use cases, including the oil spill in Saronikos Gulf and the long-term monitoring of the Port of Heraklion, clearly demonstrate the framework's capabilities in rapid disaster assessment, environmental degradation analysis, and trend identification through advanced 4D and 5D visualizations. Key environmental indicators such as shoreline change, wetland dynamics, sediment movement, and heat anomalies were successfully identified with minimal manual intervention, supporting EWS and DSS.

Performance evaluations confirmed the system’s high-quality outputs (PQR metric), effective visualization results (VisRes metric), and accurate detection of critical conditions (ICC metric), with significant improvements in processing time (TPR metric) and manageable storage requirements when configured for targeted regions. The flexible architecture, built upon open standards and NetCDF outputs, ensures compatibility with widely used GIS tools and supports data exchange through GeoServer and sFTP protocols.

Beyond its immediate applications in coastal and port environments, the ODC framework is adaptable for broader geospatial use cases, including vegetation health monitoring, urban sprawl analysis, and climate resilience assessment. Its integration with machine learning pipelines and potential for real-time data ingestion further position it as a key enabler for predictive, data-driven environmental intelligence.

Future enhancements will focus on real-time stream integration, dynamic predictive modeling, and expanding applicability to additional coastal and urban domains. Overall, the framework represents a significant contribution to the development of an interoperable and open-source foundation for harmonized environmental data processing and sustainable maritime spatial planning.

References

[1] W. Leal Filho *et al.*, "Assessing the impacts of climate change in cities and their adaptive capacity: Towards transformative approaches to climate change adaptation and poverty reduction in urban areas in a set of developing countries," *Science of the Total Environment*, vol. 692, pp. 1175–1190, 2019.

[2] Z. Mi *et al.*, "Cities: The core of climate change mitigation," *Journal of Cleaner Production*, vol. 207, pp. 582–589, 2019.

[3] A. Olabi and M. A. Abdelkareem, "Renewable energy and climate change," *Renewable and Sustainable Energy Reviews*, vol. 158, p. 112111, 2022.

[4] A. Temenos, I. N. Tzortzis, M. Kaselimi, I. Rallis, A. Doulamis, and N. Doulamis, "Novel insights in spatial epidemiology utilizing explainable AI (XAI) and remote sensing," *Remote Sensing*, vol. 14, no. 13, p. 3074, 2022.

[5] S. H. Pour, A. K. Abd Wahab, S. Shahid, M. Asaduzzaman, and A. Dewan, "Low impact development techniques to mitigate the impacts of climate-change-induced urban floods: Current trends, issues and challenges," *Sustainable Cities and Society*, vol. 62, p. 102373, 2020.

[6] K. Ravindra, P. Rattan, S. Mor, and A. N. Aggarwal, "Generalized additive models: Building evidence of air pollution, climate change and human health," *Environment international*, vol. 132, p. 104987, 2019.

[7] M. Shen, W. Huang, M. Chen, B. Song, G. Zeng, and Y. Zhang, "(Micro) plastic crisis: un-ignorable contribution to global greenhouse gas emissions and climate change," *Journal of Cleaner Production*, vol. 254, p. 120138, 2020.

[8] D. E. Parker, "Urban heat island effects on estimates of observed climate change," *Wiley Interdisciplinary Reviews: Climate Change*, vol. 1, no. 1, pp. 123–133, 2010.

[9] V. C. Gomes, G. R. Queiroz, and K. R. Ferreira, "An overview of platforms for big earth observation data management and analysis," *Remote Sensing*, vol. 12, no. 8, p. 1253, 2020.

[10] S. Kopp, P. Becker, A. Doshi, D. J. Wright, K. Zhang, and H. Xu, "Achieving the full vision of earth observation data cubes," *Data*, vol. 4, no. 3, p. 94, 2019.

[11] P. Baumann, D. Misev, V. Merticariu, and B. P. Huu, "Datacubes: Towards space/time analysis-ready data," *Service-Oriented Mapping: Changing Paradigm in Map Production and Geoinformation Management*, pp. 269–299, 2019.

[12] V. Harinarayan, A. Rajaraman, and J. D. Ullman, "Implementing data cubes efficiently," *Acm Sigmod Record*, vol. 25, no. 2, pp. 205–216, 1996.

[13] S. Sarawagi, R. Agrawal, and N. Megiddo, "Discovery-driven exploration of OLAP data cubes," in *Advances in Database Technology—EDBT'98: 6th International Conference on Extending Database Technology Valencia, Spain, March 23–27, 1998 Proceedings 6*, Springer, 1998, pp. 168–182.

[14] J. Gray *et al.*, "Data cube: A relational aggregation operator generalizing group-by, cross-tab, and sub-totals," *Data mining and knowledge discovery*, vol. 1, pp. 29–53, 1997.

[15] M. Francia, P. Marcel, V. Peralta, and S. Rizzi, "Enhancing cubes with models to describe multidimensional data," *Information Systems Frontiers*, vol. 24, no. 1, pp. 31–48, 2022.

[16] J. Leprince, C. Miller, and W. Zeiler, "Data mining cubes for buildings, a generic framework for multidimensional analytics of building performance data," *Energy and Buildings*, vol. 248, p. 111195, 2021.
[17] Y. Song, Y. Fan, X. Li, and Y. Ji, "Multidimensional visualization of transit smartcard data using space–time plots and data cubes," *Transportation*, vol. 45, pp. 311–333, 2018.
[18] G. Giuliani, B. Chatenoux, A. Benvenuti, P. Lacroix, M. Santoro, and P. Mazzetti, "Monitoring land degradation at national level using satellite Earth Observation time-series data to support SDG15–exploring the potential of data cube," *Big Earth Data*, vol. 4, no. 1, pp. 3–22, 2020.
[19] F. Miranda, L. Lins, J. T. Klosowski, and C. T. Silva, "Topkube: A rank-aware data cube for real-time exploration of spatiotemporal data," *IEEE Transactions on visualization and computer graphics*, vol. 24, no. 3, pp. 1394–1407, 2017.
[20] R. Tardío, A. Maté, and J. Trujillo, "A new big data benchmark for OLAP cube design using data pre-aggregation techniques," *Applied Sciences*, vol. 10, no. 23, p. 8674, 2020.
[21] A. Majeed *et al.*, "A big data-driven framework for sustainable and smart additive manufacturing," *Robotics and Computer-Integrated Manufacturing*, vol. 67, p. 102026, 2021.
[22] J. Han *et al.*, "Stream cube: An architecture for multi-dimensional analysis of data streams," *Distributed and Parallel Databases*, vol. 18, pp. 173–197, 2005.
[23] K. Boulil, S. Bimonte, and F. Pinet, "Conceptual model for spatial data cubes: A UML profile and its automatic implementation," *Computer Standards & Interfaces*, vol. 38, pp. 113–132, 2015.
[24] K. R. Ferreira *et al.*, "Earth Observation Data Cubes for Brazil: Requirements, Methodology and Products," *Remote Sensing*, vol. 12, no. 24, 2020, doi: 10.3390/rs12244033.
[25] A. Lewis *et al.*, "The Australian Geoscience Data Cube — Foundations and lessons learned," *Remote Sensing of Environment*, vol. 202, pp. 276–292, 2017, doi: https://doi.org/10.1016/j.rse.2017.03.015.
[26] C. Poussin, Y. Guigoz, E. Palazzi, S. Terzago, B. Chatenoux, and G. Giuliani, "Snow Cover Evolution in the Gran Paradiso National Park, Italian Alps, Using the Earth Observation Data Cube," *Data*, vol. 4, no. 4, 2019, doi: 10.3390/data4040138.
[27] B. Chatenoux *et al.*, "The Swiss data cube, analysis ready data archive using earth observations of Switzerland," *Scientific data*, vol. 8, no. 1, p. 295, 2021.
[28] G. Giuliani, B. Chatenoux, T. Piller, F. Moser, and P. Lacroix, "Data Cube on Demand (DCoD): Generating an earth observation Data Cube anywhere in the world," *International Journal of Applied Earth Observation and Geoinformation*, vol. 87, p. 102035, 2020.
[29] A. Temenos, N. Temenos, I. N. Tzortzis, I. Rallis, A. Doulamis, and N. Doulamis, "C2A-DC: A context-aware adaptive data cube framework for environmental monitoring and climate change crisis management," *Remote Sensing Applications: Society and Environment*, vol. 34, p. 101171, 2024, doi: https://doi.org/10.1016/j.rsase.2024.101171.
[30] USGS, "Earth Explorer." 2024. [Online]. Available: https://earthexplorer.usgs.gov/
[31] C. D. S. Ecosystem, "Copernicus Data Space Ecosystem | Europe's eyes on Earth." Accessed: Apr. 22, 2024. [Online]. Available: https://dataspace.copernicus.eu/
[32] NASA, "MODIS Data Hub." 2024. [Online]. Available: https://modis.gsfc.nasa.gov/data/

[33] "EURO-CORDEX." Accessed: Apr. 25, 2025. [Online]. Available: https://www.euro-cordex.net/
[34] "Home | Copernicus." Accessed: Apr. 22, 2024. [Online]. Available: https://atmosphere.copernicus.eu/
[35] CORDEX, "CORDEX experiment design for dynamical downscaling of CMIP6," Apr. 2025, Accessed: Jul. 15, 2025. [Online]. Available: https://zenodo.org/records/15268192
[36] "CORDEX domain description," Cordex. Accessed: May 27, 2025. [Online]. Available: https://cordex.org/domains/cordex-domain-description/
[37] "Sentinel-1 - Missions - Sentinel Online," Sentinel Online. Accessed: Jun. 21, 2023. [Online]. Available: https://copernicus.eu/missions/sentinel-1
[38] "Sentinel-2 - Missions - Sentinel Online," Sentinel Online. Accessed: Jun. 23, 2023. [Online]. Available: https://copernicus.eu/missions/sentinel-2
[39] "Sentinel-3," Sentinel Online. Accessed: Jun. 23, 2023. [Online]. Available: https://copernicus.eu/missions/sentinel-3
[40] "Sentinel-5P - Missions - Sentinel Online," Sentinel Online. Accessed: Jun. 23, 2023. [Online]. Available: https://copernicus.eu/missions/sentinel-5p
[41] "USGS EROS Archive - Landsat Archives - Landsat 1-5 Multispectral Scanner (MSS) Level-1 Data Products | U.S. Geological Survey." Accessed: May 28, 2025. [Online]. Available: https://www.usgs.gov/centers/eros/science/usgs-eros-archive-landsat-archives-landsat-1-5-multispectral-scanner-mss-level
[42] "USGS EROS Archive - Landsat Archives - Landsat 4-5 Thematic Mapper (TM) Level-1 Data Products | U.S. Geological Survey." Accessed: May 28, 2025. [Online]. Available: https://www.usgs.gov/centers/eros/science/usgs-eros-archive-landsat-archives-landsat-4-5-thematic-mapper-tm-level-1-data
[43] "Landsat 7 | U.S. Geological Survey." Accessed: May 28, 2025. [Online]. Available: https://www.usgs.gov/landsat-missions/landsat-7
[44] "USGS EROS Archive - Landsat Archives - Landsat 8-9 Operational Land Imager and Thermal Infrared Sensor Collection 2 Level-1 Data | U.S. Geological Survey." Accessed: May 28, 2025. [Online]. Available: https://www.usgs.gov/centers/eros/science/usgs-eros-archive-landsat-archives-landsat-8-9-operational-land-imager-and
[45] "MODIS Web." Accessed: Jun. 22, 2023. [Online]. Available: https://modis.gsfc.nasa.gov/about/
[46] "Sentinels Toolboxes." Accessed: May 28, 2025. [Online]. Available: https://sentiwiki.copernicus.eu/web/sentinels-toolboxes
[47] "JohnCrabs / OceanidsDataCube · GitLab," GitLab. Accessed: May 28, 2025. [Online]. Available: https://gitlab.com/JohnCrabs/oceanids-data-cube-app
[48] "Using the USGS Landsat Level-1 Data Product | U.S. Geological Survey." Accessed: Jun. 25, 2023. [Online]. Available: https://www.usgs.gov/landsat-missions/using-usgs-landsat-level-1-data-product
[49] P. E. Z. Makatounis, A. I. Stamou, and N. P. Ventikos, "Modeling the Agia Zoni II tanker oil spill in Saronic Gulf, Greece," *Marine Pollution Bulletin*, vol. 194, p. 115275, Sep. 2023, doi: 10.1016/j.marpolbul.2023.115275.
[50] I. Kavouras, I. Rallis, N. Doulamis, and A. Doulamis, "Ocean-DC: An analysis ready data cube framework for environmental and climate change monitoring over the port areas," in *Proceedings of the 17th International Conference on PErvasive Technologies Related to*

Assistive Environments, Crete Greece: ACM, Jun. 2024, pp. 412–419. doi: 10.1145/3652037.3663913.

[51] T. Acuña-Ruz *et al.*, "Anthropogenic marine debris over beaches: Spectral characterization for remote sensing applications," *Remote Sensing of Environment*, vol. 217, pp. 309–322, Nov. 2018, doi: 10.1016/j.rse.2018.08.008.

[52] R. Milewski *et al.*, "Analyses of the Impact of Soil Conditions and Soil Degradation on Vegetation Vitality and Crop Productivity Based on Airborne Hyperspectral VNIR–SWIR–TIR Data in a Semi-Arid Rainfed Agricultural Area (Camarena, Central Spain)," *Remote Sensing*, vol. 14, no. 20, Art. no. 20, Jan. 2022, doi: 10.3390/rs14205131.

[53] H. A. de A. Queiroz, R. M. Gonçalves, and M. Mishra, "Characterizing global satellite-based indicators for coastal vulnerability to erosion management as exemplified by a regional level analysis from Northeast Brazil," *Science of The Total Environment*, vol. 817, p. 152849, Apr. 2022, doi: 10.1016/j.scitotenv.2021.152849.

[54] S. C, H. Alsolai, R. Allafi, and M. A. Arasi, "Integrated image segmentation techniques for high-resolution coastal habitat mapping: Advancing remote sensing for coastal ecosystem assessment," *Journal of South American Earth Sciences*, vol. 159, p. 105526, Jun. 2025, doi: 10.1016/j.jsames.2025.105526.

[55] A.-L. Balogun, S. T. Yekeen, B. Pradhan, and O. F. Althuwaynee, "Spatio-Temporal Analysis of Oil Spill Impact and Recovery Pattern of Coastal Vegetation and Wetland Using Multispectral Satellite Landsat 8-OLI Imagery and Machine Learning Models," *Remote Sensing*, vol. 12, no. 7, Art. no. 7, Jan. 2020, doi: 10.3390/rs12071225.

[56] I. Kavouras, E. Sardis, E. Protopapadakis, I. Rallis, A. Doulamis, and N. Doulamis, "A low-cost gamified urban planning methodology enhanced with co-creation and participatory approaches," *Sustainability*, vol. 15, no. 3, p. 2297, 2023.

[57] I. Kavouras, I. Rallis, E. Sardis, E. Protopapadakis, A. Doulamis, and N. Doulamis, "Empowering Communities Through Gamified Urban Design Solutions," *Smart Cities*, vol. 8, no. 2, Art. no. 2, Apr. 2025, doi: 10.3390/smartcities8020044.

END OF DOCUMENT